THESIS FOR THE DEGREE OF DOCTOR OF PHILOSOPHY

Surfactant–Chelating Agent Interplay: Effect on Self-Assembly, Surface Properties, and Performance

Josmary Velásquez Cano

Department of Chemistry and Chemical Engineering

Chalmers University of Technology

Gothenburg, Sweden, 2026

Surfactant–Chelating Agent Interplay:
Effect on Self-Assembly, Surface Properties, and Performance
JOSMARY VELASQUEZ
ISBN 978-91-8103-369-4

Acknowledgements, dedications, and similar personal statements in this thesis reflect the author's own views.

Doktorsavhandlingar vid Chalmers tekniska högskola
Ny serie nr 5826
ISSN 0346-718X
https://doi.org/10.63959/chalmers.dt/5826

Department of Chemistry and Chemical Engineering
Chalmers University of Technology
SE-412 96 Gothenburg
Sweden
Telephone + 46 (0)31-772 1000

This work was financially supported by the Swedish Foundation for Strategic Research and Nouryon Surface Chemistry AB.

Cover:
The cover illustrates a schematic representation of spherical mixed micelles formed by nonionic and linear amphoteric surfactants in the presence of a chelating agent. The linear amphoteric surfactant interacts with the chelating agent and is incorporated into the mixed micelles, while branched amphoteric surfactants interact with the chelating agent but remain predominantly in the bulk solution, together with an excess of free chelating agent molecules.

Printed by Chalmers Digitaltryck
Gothenburg,
Sweden, March 2026

Surfactant–Chelating Agent Interplay: Effect on Self-Assembly, Surface Properties, and Performance

JOSMARY VELASQUEZ CANO
Department of Chemistry and Chemical Engineering
Chalmers University of Technology

Abstract

Chelating agents are common components of aqueous surfactant formulations, yet they are typically regarded as passive additives whose role is limited to metal ion sequestration. This thesis challenges that assumption by showing that chelating agents such as glutamate diacetate and methylglycinediacetate actively interact with mixed surfactant systems and significantly influence micellar organization, dynamics, and formulation cleaning performance.

A systematic multi-scale investigation was conducted using mixed surfactant systems composed of nonionic and amphoteric surfactants with varied hydrophobic chain architectures. Diffusion NMR spectroscopy, small angle neutron scattering (SANS), cloud point measurements, viscosity analysis, and interfacial performance tests were employed to probe molecular dynamics, mesoscopic structure, and macroscopic behavior.

Diffusion NMR demonstrates that chelating agents undergo dynamic association with micellar environments, despite not forming aggregates themselves. Complementary SANS measurements reveal that this association is accompanied by changes in micellar size, shape, and internal organization, with the extent of restructuring strongly dependent on surfactant architecture, particularly hydrophobic chain branching. Linear amphoteric surfactants form mixed micelles that readily reorganize upon chelating agent addition, whereas branching reduces packing adaptability and limits structural response.

The macroscopic properties reflect these molecular interactions. Cloud point and viscosity measurements identify regimes in which chelating agents counteract classical salting-out behavior, particularly in amphoteric-stabilized systems. Changes in wetting, cleaning efficiency, and foam stability further demonstrate that chelating agent concentration governs the redistribution of surfactant between bulk and interfacial regions through micellar reorganization.

Complementary SANS measurements reveal that this association is accompanied by changes in micellar size, shape, and internal organization, with the extent of restructuring strongly dependent on surfactant architecture, particularly hydrophobic chain branching. Linear amphoteric surfactants form mixed micelles that readily reorganize upon chelating agent addition, whereas branching reduces packing adaptability and limits structural response.

Keywords: chelating agents, surfactant interactions, micellar structure, diffusion NMR, formulation behavior.

Scientific Contribution

The research carried out has resulted in five papers that together explore how the structure of amphoteric surfactants and chelating agents influences their interactions, self-assembly behavior, and macroscopic performance in solution and in formulations. These papers are listed below.

Paper I. **The role of chelating agent in the self-assembly of amphoteric surfactants**

Josmary Velásquez, Lars Evenäs, and Romain Bordes.
Journal of Colloid and Interface Science, 2024, vol. 676, p. 1079-1087.

Paper II. **Amphoteric surfactant-chelating agents interactions: Impact on bulk and surface properties**

Josmary Velásquez, Sarah Lundgren, Lars Evenäs, and Romain Bordes.
Journal of Colloid and Interface Science, 2025, vol. 694, p. 137606.

Paper III. **Tail branching in mixed ionic/nonionic surfactant systems with chelating agents. Effect of branching of the ionic surfactant**

Josmary Velásquez, Alexander Idström, Lars Evenäs, and Romain Bordes.
Submitted.

Paper IV. **Tail branching in mixed ionic/nonionic surfactant systems with chelating agents. Combined branching of amphoteric and nonionic surfactants**

Josmary Velásquez, Clémence Le Coeur, Lorenzo Metilli, Anne-Laure Fameau, Lars Evenäs, and Romain Bordes.
Manuscript.

Paper V. **Amphoteric surfactant–chelating agent interactions governing emulsification, foaming, and cleaning behavior**

Josmary Velásquez, Lars Evenäs, and Romain Bordes.
Submitted.

I am the main author of all included papers and responsible for data interpretation, visualization, writing, and editing across all papers. I conducted all experimental work in most cases, except for the following specific measurements: surface tension and contact angle measurements in binary systems in Paper II, the diffusion NMR measurement for the system containing the branched amphoteric surfactant in Paper III, and the SANS experiments and related data processing in Paper IV. I also produced the graphical artwork inspired by Paper II that was selected by the Journal of Colloid and Interface Science for publication on the inside back cover of volume 696.

The work presented in this thesis has been disseminated broadly within the scientific community. Between 2023 and 2025, I presented my research as oral contributions at several international conferences each year, including Formula XI, Formula XII, ECIS, SwedNMR, Jornadas de Fisicoquímica, and Sepawa. In 2024, I was invited to deliver a keynote presentation at the ECIS Conference, where I presented results on chelating agent–surfactant interactions and their impact on macroscopic formulation properties.

Table of Contents

CHAPTER 1

Introduction

Cleaning is the process of removing unwanted substances, such as dirt, infectious agents, and other impurities, from a surface. It is conducted in various contexts and employs numerous methods. Detergency refers to the process by which formulations of surface-active agents, commonly called detergents, are used to lift and displace unwanted deposits. In a typical cleaning process, there are multiple components: the object to be cleaned (substrate), the soil or unwanted deposit to be removed, the cleaning solution applied to the substrate, and often an input of energy in the form of a mechanical or thermal action. Each of these components can vary in terms of properties, composition, and method of application.

The detergency process is inherently complex, due to the diverse and intricate nature of both soils and surfaces involved. Soils can be categorized into three types according to their chemistry: organic, inorganic, or a combination thereof. Organic soils, including food residues (such as fats, proteins, and carbohydrates), living organisms (like mold and bacteria), and petroleum-based substances (such as motor oil), are traditionally removed using alkaline cleaners, solvents and/or surfactants.

Inorganic soils, such as rust, mineral deposits, and scale, often require acidic or specialized cleaners to remove them effectively. The most challenging soils are of combined nature, which contain both organic and inorganic elements.

In addition to soil complexity, surface characteristics, such as roughness, porosity, and texture, affect the cleaning process, thereby influencing the adhesion between the soil and surface. The strength of this adhesion depends on factors like wettability and molecular interactions, making it particularly challenging to remove soils when they share similar polarity with the surface.

Surfactants are central to detergent formulations, their amphiphilic nature (possessing affinity for both hydrophilic and hydrophobic environments) allows them to migrate to interfaces and to decrease surface free energy, facilitating soil removal. The role of surfactants in influencing surface free energy and their relation to cleaning processes are presented in the section "Physicochemical Principes of Detergency."

To achieve effective cleaning, formulations typically combine multiple ingredients beyond surfactants, including solubilizers and chelating agents. Solubilizers serve as coupling agents, integrating surfactants, solvents, and inorganic salts into a homogeneous solution. Chelating agents bind to divalent ions, enhancing the cleaning action of detergents.

The functions required of other essential ingredients in cleaning formulations are continuously evolving, shaped not only by technical needs but also by the practices and preferences of detergent producers and the regions in which they operate. One key aspect of this field is the availability of multiple, nearly equivalent technical solutions to achieve the desired outcomes. In this context, achieving the required function takes precedence, while the choice of ingredients is only one part of the process.[1–3] Often, different products or systems can be proposed to meet the same specifications with similar efficacy. For instance, hydrotropes and secondary surfactants can both be used to improve solubility, and

similarly, chelating agents and some polymers can both be applied to control water hardness and prevent redeposition. The focus of this work will be on hydrotropes, secondary surfactants, and strong chelating agents, which play critical roles in cleaning formulations. Each of these components will be discussed in separate sections.

Although chelating agents are indispensable components of cleaning formulations, their broader effects within surfactant systems remain poorly understood. Traditionally regarded as inert additives, their potential influence on surfactant aggregation and interfacial behavior is rarely considered, and most models treat them as non-interacting species. However, this assumption overlooks the possibility that chelating agents may actively modulate micellization, interfacial organization, or solubilization processes.

Practical formulation studies have revealed that specific combinations of amine-based surfactants with aminopolycarboxylate chelating agents can produce concentrated and stable cleaning products; something not achievable with alternative surfactant or chelating agent chemistries. These observations suggest a distinct type of molecular interaction that influences aggregation and phase behavior. To understand the origin of this effect, the present work investigates the interactions between amine-based surfactants and chelating agents, examining their molecular characteristics and their effects on the bulk and surface properties of surfactant-based cleaning formulations.

The techniques used to evaluate these interactions and their effects on surface and macroscopic properties are described in the experimental section. Molecular interactions between surfactants and chelating agents were examined by NMR spectroscopy, focusing on changes in chemical shift, line shape, and self-diffusion behavior to gain insight into complex formation and molecular dynamics. Dynamic Light Scattering (DLS) and Small-Angle Neutron Scattering (SANS) measurements were employed to characterize variations in micellar size, shape, and internal structure induced by chelating agents. To link these

molecular-level observations with macroscopic performance, key formulation properties such as surface tension, contact angle, cloud point, viscosity, and foaming were systematically evaluated, and their correlation with cleaning efficiency was established.

Purpose and Objectives

This study explores the interactions between surfactants and aminopolycarboxylic chelating agents, a relatively underexplored area despite their widespread industrial use. By gaining a deeper understanding of these systems, it is possible to design formulations that capitalize on these interactions to reduce salting-out effects, enhance the solubility of complex surfactant mixtures, and control surface properties. Ultimately, the goal is to provide insights that will guide the development of more efficient and sustainable cleaning formulations for various industrial applications.

The objectives of this work were organized into four main areas:

(i) establishing the existence and general characteristics of surfactant–chelating agent interactions,

(ii) evaluating the influence of hydrophilic group chemistry on these interactions,

(iii) examining the effect of lipophilic chain architecture in single and mixed surfactant systems, and

(iv) assessing the macroscopic consequences of these interactions for formulation properties.

To achieve these objectives, the work was organized into four thematic areas, with each objective addressed through one or more papers:

(i) General features of surfactant–chelating agent interactions. Paper I establishes the presence and dynamic nature of interactions between amine-based surfactants and aminopolycarboxylate chelating agents. NMR spectroscopy was used as the primary tool to

identify and characterize these interactions, with particular focus on chemical-shift changes as a function of surfactant concentration. Diffusion NMR was employed to distinguish molecular species in solution and to identify changes in mobility associated with the formation of assemblies.

(ii) Effect of hydrophilic group chemistry. Paper II investigates how variations in the surfactant head-group structure and the type of chelating agent influence the strength and nature of the interactions. A series of amine-based surfactants combined with polycarboxylic acid-type chelating agents was studied using ^{13}C NMR line-shape analysis and chemical-shift behavior. This study highlights how the nature of both the surfactant head-group and the chelating agent modulates the association.

(iii) Effect of lipophilic chain architecture. The role of hydrophobic structure was examined in Papers III and IV, both of which employed mixed surfactant systems containing an amphoteric and a nonionic surfactant. Paper III evaluates how changes in the lipophilic chain architecture of the amphoteric surfactant influence the surfactant–chelating agent interaction, while the structure of the nonionic surfactant is kept constant. Cloud point, viscosity, diffusion NMR, and DLS were used to assess changes in aggregation behavior and solution structure. Paper IV builds on this analysis by systematically varying the hydrophobic chain architecture of both amphoteric and nonionic surfactants, thereby revealing cooperative effects within mixed micellar systems. Changes in micellar geometry and molecular mobility were probed using SANS and diffusion NMR, respectively. Collectively, these results demonstrate how lipophilic chain design controls chelating-agent association in mixed surfactant formulations.

(iv) Macroscopic formulation behavior. The macroscopic implications of surfactant–chelating agent interactions, including effects on cloud point, viscosity, surface tension, contact angle, foaming, and cleaning performance, were evaluated throughout the work.

Paper V provides an application-oriented perspective, examining how these interactions influence the performance and stability of typical cleaning formulations. Together, these studies link molecular-level interactions to formulation behavior relevant to industrial practice.

CHAPTER 2

Physicochemical Principles of Detergency

Effective detergency relies on several processes occurring simultaneously and synergistically. First, the cleaning solution must wet both the substrate and the soil, altering the interfacial properties at phase boundaries within the system. Simultaneously, simple solvation or liquid mediated removal of the dirt may occur. In many cases, mechanical agitation, such as rubbing or shaking, provides shearing action that helps detach the soil from the substrate and promotes mass transfer within the system. Once the soil leaves the surface, it must be suspended, solubilized, or emulsified by the cleaning solution. Finally, the contaminated solution is removed (*e.g.*, by rinsing or wiping) to prevent redeposition on the surface.

Surfactants and chelating agents are crucial in detergent formulations. Simple cleaning products, like window cleaners, may rely solely on these two ingredients. However, more sophisticated formulations often contain a range of additives that improve cleaning performance and deliver specific benefits. Enzymes, for instance, are added to facilitate the hydrolysis of

specific soils, bleaching agents to remove colored stains, and optical brighteners to enhance whitening. Polymers prevent soil redeposition and inhibit crystal growth. Perfumes, dyes, and foam control agents adjust the sensory and functional properties of the product, while solubilizers help to integrate the different ingredients into a homogeneous solution. All ingredients are contributing to the overall efficacy of the detergent solution.

This thesis focuses on understanding the physicochemical behavior and molecular interactions in simple cleaning formulations, such as the one described in the previous paragraph. The following sections will describe the key ingredients in cleaning products and explore their mechanisms of action, starting with surfactants and correlating their physicochemical properties to each stage of the cleaning process.

2.1 Surfactants

A typical detergent formulation relies heavily on surfactants, amphiphilic molecules that contain both hydrophilic (water-loving) and hydrophobic (water-repelling) moieties. This dual affinity drives surfactants to migrate to interfaces, such as water-air or water-oil boundaries, resulting in a change in surface free energy. In this context, the terms "hydrophilic" and "hydrophobic" can also be referred to as "lipophobic" (fat-repelling) and "lipophilic" (fat-loving), respectively.

Surfactants consist of an alkyl chain, typically with 8–22 carbon atoms, and a functional head group that interacts with water. Based on the head group, surfactants are classified as ionic or nonionic. Ionic surfactants dissociate into ions in water and are further divided into anionic, cationic, zwitterionic and amphoteric. Anionic surfactants have a negatively charged head group, while it is positively charged for cationic surfactants. Zwitterionic surfactants bear both positive and negative charges on the head group, whereas amphoteric surfactants change their ionization state with the pH of the solution. Nonionic surfactants

have no ionic charge and therefore do not ionize in water. In detergent formulations, anionic and nonionic surfactants have historically been the most widely used, with nonionic surfactants being employed for their ability to emulsify oils and remove organic soils.

2.1.1 Surfactant Solubility and Phase Separation

The solubility of surfactants in different solvents is governed by several interrelated parameters. One of the primary factors is the structure of the surfactant, particularly the balance between its hydrophilic and lipophilic moieties. Surfactants with larger hydrophobic chains and smaller or less polar hydrophilic groups tend to have reduced water solubility but are more soluble in non-polar solvents. This structural balance directly influences the behavior of the surfactant in different solvent environments, determining its partitioning between water and oil.

Temperature is another critical factor that affects surfactant solubility, and two concepts are widely used to describe this dependence: the Krafft temperature and the cloud point. The Krafft temperature, typically relevant to ionic surfactants, refers to the temperature below which surfactant molecules, when in a solution above the CMC, form insoluble hydrated solids with crystalline features. Above this temperature, the molecules form micelles.

While the solubility of many ionic surfactants increases with rising temperature, nonionic surfactants containing polyoxyethylene chains behave differently, showing decreased solubility as temperature increases. This is described by the cloud point, the temperature above which the surfactant solutions (typically measured at 1 wt%) separate into a surfactant-rich phase and a dilute aqueous phase, initially visible as cloudiness. The onset of turbidity is influenced by factors like polyoxyethylene chain length and, to a lesser extent, the hydrophobic chain length, as well as surfactant concentration and cosolutes. There are two widely accepted models to explain this behavior.[4]

The first model attributes solubility to the formation of hydrogen bonds between water molecules and ether oxygen in the ethylene oxide chain. As temperature increases, these bonds weaken, leading to dehydration of the polyoxyethylene chains and decreased solubility.

The second model emphasizes the conformational flexibility of polyoxyethylene chains, which can adopt various structural forms with different energies and polarities. At lower temperatures, a low-energy, highly polar conformation dominates, promoting interactions with water. With increasing temperature, higher-energy, less polar conformations become more prevalent, reducing polarity and consequently hydration. This shift favors stronger surfactant-surfactant interactions, closer head group packing, and an increased tendency for phase separation.

The Krafft point concept is generally not relevant for cleaning applications because the presence of impurities or additives in cleaning formulations lowers the Krafft point, much like solutes depress the freezing point of a solvent. In practice, this means the Krafft point for cleaning products is always below standard operating temperatures, making it less of a concern. In contrast, the cloud point is of critical importance. It affects both product shelf stability and cleaning efficiency. Cleaning formulations are typically designed so that the cloud point is above room temperature, ensuring that the formulation remains stable and well-dispersed during storage. At the same time, the cloud point should be just above the optimal cleaning temperature, as numerous studies indicate that detergency is most effective near, but below, this threshold.[5,6] This balance maximizes both product stability and cleaning performance, making the cloud point a key consideration in detergent formulation.

2.1.2 Adsorption and Surface Activity

The amphiphilic nature of surfactants drives their adsorption at interfaces such as air–water or oil–water interfaces. When surfactant molecules migrate to these interfaces, they arrange themselves in a specific orientation: their hydrophilic heads face the aqueous phase, while their hydrophobic tails are oriented away from water. This process is driven by a reduction in free energy, as removing the hydrophobic segments from the aqueous environment minimizes the energetic penalty associated with accommodating nonpolar moieties in water, a phenomenon known as the hydrophobic effect.[4,6,7]

At air-water or oil-water interfaces, the orientation of surfactants is relatively straightforward: the hydrophilic head group faces the water, while the lipophilic tail extends into the second phase. However, the adsorption of surfactants at surfaces other than air, such as solid or oil/water interfaces, is more complex, as the process is influenced not only by the hydrophobic effect but also by the energy gained when interactions between the surface and surrounding water are replaced with interactions between the surface and surfactant molecules. As a result, the nature of the solid surface, in combination with the type of surfactant, determines both how the surfactant molecules adsorb and the morphology of the adsorbed layer.

One of the key effects of surfactant adsorption is the reduction of interfacial tension. Interfacial tension refers to the cohesive forces at the boundary between a liquid and another phase, such as air (denoted surface tension) or another non-miscible liquid such as an oil. Molecules at the surface of the liquid experience fewer cohesive forces than those in the bulk, due to the lack of neighboring molecules on one side; this imbalance in interaction results in a greater tendency for the molecules at the surface to interact with their neighboring molecules (Figure 1). In a solid, the excess energy is referred to as surface free energy.

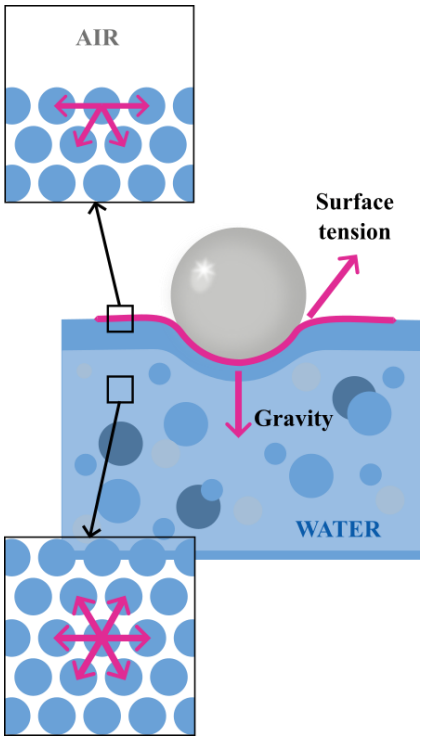

Figure 1. Illustration of surface tension at the liquid-air interface, highlighting the imbalance of cohesive forces experienced by molecules at the surface compared to those in the bulk. This results in higher energy for surface molecules.

When surfactants are introduced in water, they align at the interface, where interactions between the surfactant head groups and water molecules, along with van der Waals forces between the hydrophobic tails and the second phase (lipophilic, such as solid or oil), or between the tails themselves (if the second phase is air), balance the forces at the interface. These increased interactions at the interfacial region result in a decrease in the interfacial tension.

2.1.3 Wetting

Wetting refers to the ability of a liquid to spread over a surface, displacing a second fluid, such as air. The extent to which a liquid spreads, known as wettability, depends on the properties of both the liquid and the surface. Wettability is governed by two types of forces: adhesive forces between the liquid molecules and the surface, promoting wetting, and cohesive forces within the liquid, which encourage the liquid to bead up. The balance between these forces determines whether the liquid wets the surface or forms a droplet, and correlates with the interfacial energy of the liquid, the fluid and the surface.

To quantify wettability, the contact angle (θ) formed between the liquid and solid surface can be measured (Figure 2). According to Young's equation, this

contact angle is related to the surface free energies between the solid, liquid, and the surrounding fluid (often air).

A smaller contact angle indicates better wetting, with water angle less than 90° suggesting favorable wetting, meaning that the liquid spreads more across the surface. Conversely, a contact water angle greater than 90° implies poor wetting, where the liquid tends to minimize its contact with the surface, forming a more spherical droplet.

By lowering the interfacial tension at the interfaces between pairs of components—such as the detergent solution and the soil or the detergent solution and the solid surface—the adhesive forces binding the soil to the surface are diminished, facilitating its removal.

$$\cos\theta = \frac{\gamma_{SG} - \gamma_{SL}}{\gamma_{LG}}$$

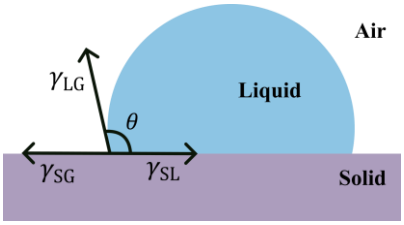

Figure 2. Contact angle measurement illustrating the variables in the Young's equation. The contact angle (θ) is shown at the interface where a liquid droplet meets a solid surface, with forces represented as surface tensions at the liquid-solid (γ_{SL}), liquid-vapor (γ_{SG}), and solid-vapor (γ_{LG}) interfaces. The Young equation relates these forces to determine the equilibrium contact angle.

2.1.4 Micellization

When a surfactant is added to water, it is initially present as single entities, or unimers, dissolved in the solution. As introduced earlier, the hydrophobic portion of each unimer disrupts the water structure, raising the free energy of the system. To counteract this, unimers migrate to interfaces, accommodating their lipophilic chains by orienting them away from the water. Another way to reduce free energy is through self-association, where unimers form micelles,

incorporating the hydrophobic groups inward while the hydrophilic heads face the solvent. However, adsorption and micellization involve trade-offs, such as restricted molecular freedom and, for ionic surfactants, electrostatic repulsion within the micelle, which counteract this tendency. Ultimately, the occurrence and concentration above which micellization appears, reflect the balance between forces that promote and oppose self-association.

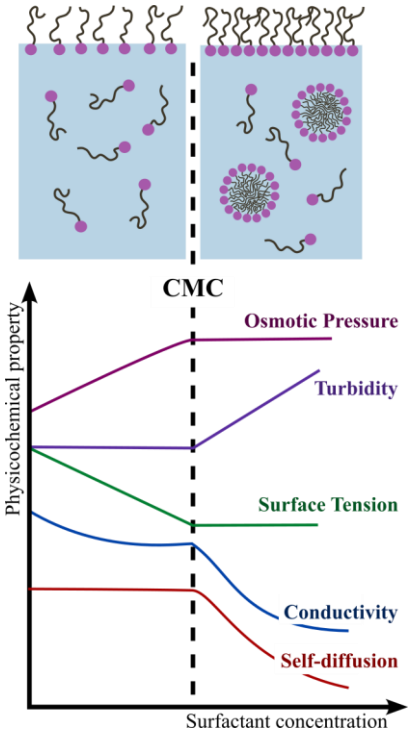

Figure 3. Plot illustrating changes in physicochemical properties, such as viscosity, surface tension, and turbidity, as surfactant concentration increases. The accompanying sketches depict the micellization process: at low concentrations, surfactant molecules are dissolved as individual units, while at higher concentrations, beyond the CMC, they aggregate into micelles.

Micellization can be demonstrated by measuring various physicochemical properties of the solution as the surfactant concentration increases. At the point of micelle formation, nearly all measurable physical properties of solutions undergo a sharp change (Figure 3), particularly those associated with the size or number of entities in solution, such as conductivity, light scattering, or osmotic pressure. This behavior is unique to systems undergoing self-association, other solutes show gradual changes in the properties as the concentration increases. This specific concentration above which self-association takes place is known as the critical micelle concentration (CMC), often determined by evaluating changes in surface tension.

While spherical micelles are the most commonly observed structures, surfactant molecules can self-

assemble into a variety of geometries, including rod-like micelles, vesicles, and others. The shape of these aggregates is largely determined by the interactions between the surfactants, as a consequence of the molecular structure, and this relationship can be described using the Critical Packing Parameter (CPP). The CPP is calculated as:

$$\mathrm{CPP} = \frac{v}{a_0 \cdot l} \qquad (1)$$

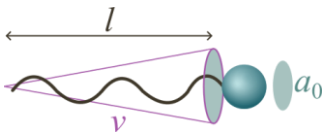

where v is the volume of the surfactant tail, l the length of the surfactant tail, and a_0 the surface area of the hydrophilic headgroup at the aggregate surface. It is well established that a CPP value of 1/3 yields spherical micelles, 1/2 cylindrical micelles, 1 lamellar micelles, and values greater than 1 give reverse micelles. This parameter links molecular shape and corresponding interactions to aggregate geometry, influencing bulk properties such as the viscoelasticity of the solution[8] and solubilization capacity.[9]

Above CMC, micelles and unimers coexist in a dynamic equilibrium, where surfactant molecules continuously associate and dissociate from micelles. In this manner, micelles act as a reservoir of surfactant molecules, ready to migrate to new surfaces as they appear, such as when a surfactant solution spreads over a solid substrate.

2.1.5 Micellar Solubilization

When a third component, such as a hydrocarbon, is added to an aqueous surfactant solution, its behavior depends on the presence and type of micelles. Below the CMC, the solubility of the additive is similar to its solubility in water. Above the CMC, however, the solubility of the hydrophobic compound often increases significantly. For non-polar compounds like oils, micelles swell by incorporating some of the oil, allowing solubilization to occur within the lipophilic core of the micelle.

An important variable in the solubilization of oily matter in micellar systems is therefore the concentration of surfactant. Soil removal only becomes significant above the CMC,[10,11] and reaches its maximum at concentrations several times the CMC. At high surfactant concentrations (10-100 times the CMC), a substantial amount of oily matter can be solubilized, whereas at lower surfactant concentrations, only minor quantities of oil are solubilized. In the latter case, the remaining oil must be suspended in the solution in the form of a dispersion, *e.g.* as an emulsion, a topic that will be discussed later. Therefore, it is essential that surfactant concentrations in cleaning formulations exceeds the CMC by several orders of magnitude to guarantee that micelles are present in sufficient quantities.

Solubilization in micellar systems is influenced not only by the nature of the additive, but also by several formulation parameters, such as temperature, electrolyte concentration, and surfactant type. For instance, nonionic ethoxylated surfactants exhibit greater affinity for oil as temperature increases, leading to the formation of oil-in-water emulsions at lower temperatures and water-in-oil emulsions at higher temperatures. The temperature at which this inversion occurs is known as the Phase Inversion Temperature (PIT). At the PIT, the oil-water interfacial tension reaches a minimum, leading to maximum solubilization of non-polar materials. For both polyoxyethylene nonionic surfactants and polyoxyethylene nonionic-anionic mixtures the optimal oily soil detergency has been correlated with the

PIT.[12,13] There is also a notable correlation between the PIT in emulsions and the cloud point in solutions of nonionic ethoxylated surfactants, which also extends to cleaning performance.[14–16]

2.1.6 Dispersions

A dispersion refers to a system where small particles, droplets, or bubbles of one substance are distributed throughout another substance, the continuous phase, typically through mechanical energy input such as stirring or agitation. In cleaning processes, the main types of dispersions are emulsions, suspensions, and foams.

Emulsions:

An emulsion involves two immiscible liquids, oil and water, where one liquid is dispersed as tiny droplets within the other. The main difference between micellar solubilization and emulsions is that micellar solubilization is thermodynamically stable, while emulsions can only be kinetically stable; it implies that an energy input is required. Without stabilization, the liquids in an emulsion would quickly separate, *i.e.* they return to their original state before homogenization. To create a stable emulsion, an emulsifying agent, typically a surfactant, is used. Surfactants reduce the interfacial tension between the two liquids, allowing the droplets to form at lower energetic cost. Additionally, surfactants form an interfacial film around the droplets that prevents them from coalescing immediately. The stability of an emulsion depends on the strength of this film and the reduction of interfacial energy, which can be enhanced by adding fine particles or creating steric and electrostatic barriers to prevent droplet coalescence.

Suspensions:

A suspension is a dispersion where non-soluble solid particles are distributed in a liquid phase. The stability of the suspension is a concern, as particles tend to settle or agglomerate without proper stabilization. To prevent this, electrostatic barriers are formed by adsorbing

similarly charged ions or surfactants onto the particle surfaces, creating repulsion between particles. Additionally, steric barriers created by bulky molecules, such as non-ionic surfactants with long hydrophilic head groups or polymers, can prevent aggregation by forming a stabilizing layer around them, giving rise to repulsive interactions of both steric and osmotic origin.

Foams:

Foams are dispersions of gas in a liquid or solid; the focus of this work is on liquid foams. These are systems in which gas bubbles are trapped within a thin liquid film. Like emulsions and suspensions, foams are inherently unstable. Owing to the large density difference between the gas and liquid phases, gravitational effects are especially pronounced in foams compared to emulsions.

In the context of cleaning formulations, emulsions, suspensions, and foams serve as a medium to carry away dirt that has been removed from surfaces during cleaning. Foams, besides being a carrier, also enhance the sensory properties of cleaning formulations, making them more appealing to users. In household applications, foaming is associated by consumers with the quality of the cleaner and provides visual clues on the performance of cleaning products. In industrial and institutional (I&I) settings, foaming can bring benefits such as low-water cleaning and improved adhesion to vertical surfaces. However, many I&I cleaning processes require low-foaming formulations, especially when mechanical energy is involved, to prevent issues like pressure build-up or difficulties in rinsing large amounts of foam, which can flood industrial areas.

2.1.7 Effect of the Chemical Structure of Surfactants on Surface Properties

The behavior of surfactants in solution and at interfaces is governed by the balance between their hydrophilic and hydrophobic structural elements. Changes in the size, shape, and positioning of these groups influence adsorption at interfaces, micellization behavior, and

ultimately performance in cleaning applications.[17,18] These structure–performance relationships reflect the underlying molecular processes that drive amphiphiles to reduce interfacial free energy and organize into interfacial films and aggregates.[19] In general terms, molecular features that enhance interfacial affinity promote rapid adsorption and efficient surface tension reduction, whereas features that favor micellization can limit the amount of monomer available for interfacial processes at higher concentrations.

Lipophilic chain length and architecture

The hydrophobic chain strongly influences surfactant efficiency and aggregation behavior. Increasing alkyl chain length enhances the hydrophobic effect, lowering the free energy of adsorption at interfaces and improving surface activity at low concentrations, while simultaneously shifting micellization to lower concentrations.

Chain branching or unsaturation disrupts the close packing of hydrophobic tails. As a result, branched or unsaturated chains tend to show slightly reduced adsorption efficiency but can achieve lower ultimate surface tensions. These structural features also enhance molecular mobility at the interface, contributing to faster dynamic surface tension reduction and improved wetting and spreading, properties that are beneficial in many cleaning processes. Conversely, longer straight-chain surfactants form more ordered films and more stable micelles, which translates into increased foam stability and stronger solubilization capacity for oily soils at equilibrium, albeit with slower interfacial equilibration.

Head-group chemistry and position

The chemistry and positioning of the hydrophilic head-group also play crucial roles in governing interfacial and aggregation behavior. Terminal head-groups favor efficient adsorption and robust micellization due to well-defined hydrophobic–hydrophilic separation. Relocating the polar group toward the middle of the chain disrupts tail packing,

increases the CMC, and reduces surface efficiency, highlighting the importance of molecular geometry in interfacial orientation.

The nature of the head-group also modulates intermolecular interactions at the interface. Ionic surfactants experience electrostatic repulsion that increases the CMC and may reduce adsorption efficiency relative to nonionic surfactants. This arises in part from an entropic penalty due to the restricted mobility and ordering of counter-ions near the interface, which can be mitigated by counter-ion association or electrolyte screening. Nonionic surfactants, stabilized primarily by hydrogen bonding and steric hydration, generally exhibit lower sensitivity to electrolytes and predictable surface tension behavior but tend to form less stable foam. Amphoteric and zwitterionic surfactants combine favorable surface activity with mildness and electrolyte tolerance, making them particularly useful as secondary surfactants in mixed systems and as formulation stabilizers in complex cleaning environments.

Overall, head-group chemistry affects not only surface adsorption and micellization but also compatibility with builders, chelating agents, and electrolytes, influencing formulation stability and cleaning performance.

Variations in surfactant tail structure and branching, along with differences in head-group chemistry, manifest in practical cleaning performance. Surfactants with shorter or branched hydrophobic chains typically promote rapid wetting and spreading, aiding soil removal on hydrophobic surfaces. Longer, linear chains enhance foam stability and micellar solubilization capacity, supporting sustained cleaning under high-soil conditions. Meanwhile, head-group chemistry governs interfacial charge, hydration, and tolerance to formulation additives, and therefore plays a critical role in optimizing detergency, foaming, emulsification, and system stability across different formulation environments.

2.1.8 Mixed Surfactant Systems

In practice, surfactants are rarely used as single-component systems. Instead, mixtures of surfactants with different head-group chemistries, hydrophobic chain lengths, and degrees of branching are commonly employed to achieve targeted performance, cost efficiency, and formulation robustness. As a result, the behavior of mixed surfactant systems is of greater relevance to real-world applications than that of pure surfactant solutions.

When multiple surfactants are present, their distribution between interfaces, micelles, and the bulk solution is governed by the differences in hydrophobicity, head-group interactions, and packing constraints. More hydrophobic surfactants preferentially populate interfaces and micellar cores, where their exposure to water can be minimized, while more hydrophilic components tend to remain in the bulk phase or occupy regions of higher curvature. This selective partitioning plays a central role in determining interfacial tension, micellar size and shape, and the overall solubility of the system.

In mixed micelles, differences in molecular geometry and hydrophobic chain architecture lead to nonideal mixing behavior. Linear surfactants often pack more efficiently within aggregates, whereas branching introduces steric constraints that increase interfacial area requirements and frustrate close packing. Although branched surfactants form micelles less efficiently, they can reduce surface tension to lower equilibrium values than linear analogues. This arises because branching allows surfactant molecules to adopt less ordered, more favorable configurations at the interface, lowering the free energy per adsorbed molecule. These effects influence not only aggregate morphology but also the response of the system to external additives, changes in ionic strength, or temperature variations.

Mixed surfactant systems are particularly sensitive to molecular additives that alter hydration, head-group interactions, or effective packing parameters, as the presence of multiple surfactant species introduces additional degrees of freedom. Even small changes

in composition can redistribute surfactant populations between bulk, micellar, and interfacial environments, leading to pronounced changes in macroscopic behavior.

Understanding how surfactant structure governs partitioning and cooperative behavior in mixed systems is therefore essential for interpreting formulation responses and for rationalizing how auxiliary components, such as chelating agents, can modulate micellar organization and interfacial properties.

2.2 Characterization of Surfactant Interactions and Aggregates

Understanding surfactant self-assembly and intermolecular interactions requires experimental techniques that probe structure and dynamics across multiple length and time scales. Because surfactant systems are inherently hierarchical and dynamic, spanning molecular-level interactions, mesoscopic aggregate structure, and macroscopic formulation properties, no single technique provides a complete description. Instead, complementary methods are commonly combined to build a coherent picture of surfactant behavior in solution.

At the molecular scale, techniques such as Nuclear Magnetic Resonance, infrared spectroscopy, and calorimetry are widely used to probe local environments, intermolecular interactions, and exchange processes. These methods provide information on hydration, head-group association, and dynamic exchange between free and aggregate-associated species.

Properties at the mesoscale, including micelle size, shape, and internal organization, are typically accessed using scattering techniques such as small-angle neutron scattering, small-angle X-ray scattering, and light scattering. These methods provide ensemble-averaged structural information and are especially powerful for detecting changes in aggregate

geometry, growth, or restructuring induced by variations in composition, temperature, or the presence of additives. When combined with contrast variation or complementary spectroscopic techniques, scattering methods can also offer insight into the spatial distribution of different components within mixed aggregates.

At the macroscopic scale, techniques that probe bulk properties of formulations are employed to relate molecular and aggregate structure to practical performance. Surface tension measurements, contact angle analysis, viscosity and rheology measurements, cloud point determination, and foaming assessments are commonly used to evaluate formulation behavior. Cleaning performance can be quantified through standardized soil removal tests, providing direct links between molecular design, aggregation behavior, and functional outcomes. Combining macroscopic measurements with molecular and mesoscale techniques allows for a comprehensive understanding of surfactant systems across all relevant length scales.

2.3 Cleaning and Soil Removal Mechanisms

Cleaning and detergency are highly complex processes, largely due to the vast variety of soils, substrates, and ingredients in cleaning formulations. The following discussion focuses on the action of surfactants on soil removal process.

In general, cleaning takes place in two equally important steps: detaching soil from the substrate and suspending the soil in solution to prevent redeposition. Soils that surfactants can remove are typically attached to the substrate either through physical adsorption (via van der Waals forces or dipole interactions) or by electrostatic forces. These soils are often further classified into particulate soil and oily soil.

Surfactants are effective in removing both types of soils, though the mechanisms involved are different.

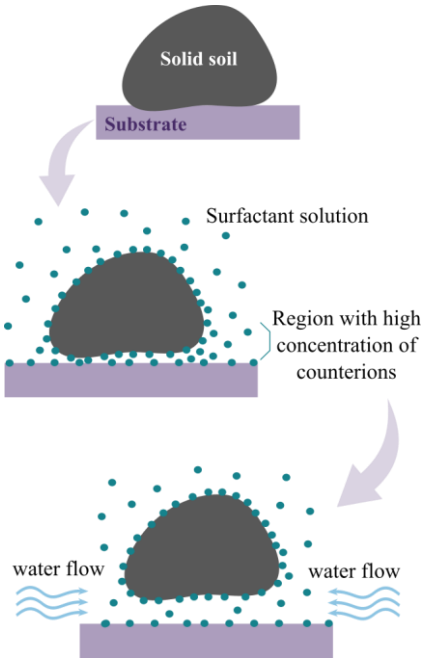

Figure 4. Mechanism of particulate soil detachment from surfaces. When both the particle and substrate have negative net charges, or like charges are induced, a diffuse layer of counterions forms, creating an osmotic flow of water into the interface. This flow facilitates the desorption of particulate soil from the surface.

Particulate soils tend to detach spontaneously when both the particle and the surface have similar net charges, which is often the case because both soils and surfaces typically carry a negative charge. If the two surfaces have opposite charges, removal is facilitated by actively inducing similar charges on both the soil and substrate surfaces. This creates a diffuse layer of counterions near the soil and substrate, which promotes an osmotic flow of water into the area, easing the desorption of solid particles (Figure 4).

A simple and effective way to induce charge formation on both soil and surface is to raise the pH of the surrounding solution. Increasing the pH can deprotonate neutral functional groups, such as carboxylic or phenolic groups, at the surfaces resulting in negative charges on both the soil and substrate; conversely acidification may protonate amines. This of course is highly dependent on the chemistry of the soil and the substrate.

Liquid soils are usually removed by the roll-back or roll-up mechanism (Figure 5) which can also apply to solid soils that can be liquefied through thermal action or by the use of additives. In this mechanism, the contact angle of the liquid soil with the surface increases as surfactant from the cleaning solution

enters the crevices between the soil and the substrate and adsorbs at both surfaces. The resulting osmotic flow may also promote the detachment of the soil, similar to the process with particulate soils described above.

For hydrophobic substrates, oily soil may wet the surface, rendering the roll-up mechanism less relevant. In that case, removal relies on reducing the interfacial tension between the oil and the surrounding water. The surfactant primarily acts on the oil-water interface, while its adsorption at the substrate-water interface plays a less important role in soil removal.

When a sufficiently low interfacial tension is achieved by the surfactant, soil removal can occur via two distinct mechanisms, which may operate independently or in parallel: micellar solubilization and emulsification (Figure 5). In both cases, the oily soil is either solubilized or dispersed in the washing liquid.

Surfactants with appropriate structure adsorb at the liquid/soil and at the solid/soil interfaces, reducing the interfacial tensions in both cases. Lower interfacial tensions reduce the energy required to detach the soil from the surface, emulsify it with mechanical action or solubilize it within micelles.

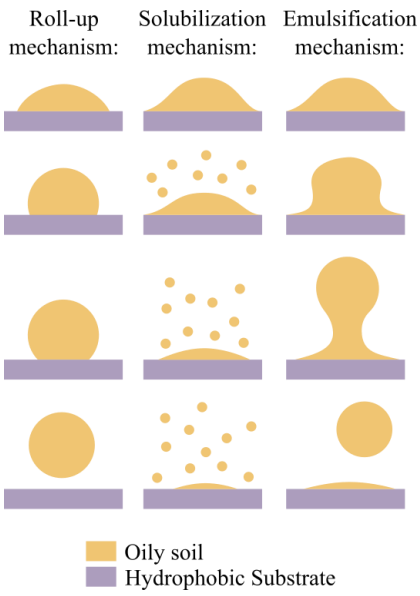

Figure 5. Mechanism of liquid soil removal from surfaces. In the roll-back or roll-up process, surfactants from the cleaning solution penetrate the crevices between the soil and substrate, increasing the contact angle of the liquid soil with the surface and creating an osmotic flow that aids in detachment. For hydrophobic substrates, however, soil removal relies on lowering the oil-water interfacial tension, allowing the surfactant to either solubilize or disperse the soil through micellar solubilization or emulsification.

In all the mechanisms mentioned above, equilibrium surface tension and surfactant adsorption values are not always reached, especially in high-speed or non-mechanical cleaning processes. In such cases, dynamic surface tension and adsorption processes become critical. Surfactants with higher diffusivity typically demonstrate superior soil removal performance under these conditions, as they are more effective at rapidly migrating to interfaces and reducing interfacial tension.[20]

It has only recently been recognized that foams can contribute directly to cleaning under specific conditions, particularly for oily residues and fine particulates. Foam-assisted cleaning arises from physical mechanisms linked to the dynamics of deformable liquid interfaces.[21–23] Three key processes are typically identified: imbibition, interfacial wiping, and drainage. Imbibition occurs when capillary pressure gradients draw soil into the foam microstructure; as liquid films and Plateau borders advance and rearrange, oils or soft contaminants are pulled into the interconnected channels of the foam network. Interfacial wiping results from the deformation, motion, and rupture of bubbles at the surface. The movement of the three-phase contact line (foam/soil/solid) and the transient micro-shear stresses generated during film sliding or bubble collapse promote detachment and lateral transport of soils, particularly thin oily layers. Drainage takes place as liquid drains through the foam under gravity or capillary forces, sweeping fine particles into thinning films and Plateau borders, where they become hydrodynamically entrained and removed from the surface.

Together, these mechanisms highlight that foam-driven cleaning is governed not only by surfactant chemistry, but also by the dynamic physics of liquid interfaces, capillary flows, and bubble rearrangements.

2.3.1 Solubilizers

A recurring challenge in the formulation of cleaning products is that the surfactants most effective for removing oily soils are also highly hydrophobic. As a result, solubilizing agents are often required to obtain a stable, single-phase detergent system in which all active ingredients remain dissolved. In industrial practice, the most common solubilizers include cosolvents, hydrotropes, and hydrophilic surfactants, here referred to as secondary surfactants. As will become apparent in the following sections, the mechanisms by which these agents promote solubilization are closely related, and the distinctions between them are often subtle, leading to some overlap and interchangeable use of terminology.

Cosolvents

Cosolvency refers to the enhancement of solute solubility in a solvent mixture through the addition of a secondary solvent (cosolvent) to the primary solvent. In most applications, a water-miscible organic solvent is introduced into an aqueous medium to increase the solubility of a poorly water-soluble compound.[24,25]

Cosolvents are characterized by their miscibility with the primary solvent and their ability to alter key solvent properties, including polarity, dielectric constant, hydrogen-bonding network, and solvation-shell structure. Common examples include ethanol, propylene glycol, glycerin, and polyethylene glycols.[26]

Several mechanisms have been proposed to explain cosolvency, including:

1. Modification of solvent polarity and dielectric constant. The addition of a less polar but water-miscible organic solvent lowers the overall polarity and dielectric constant of the medium, thereby reducing the free-energy barrier for solvating non-polar solutes and increasing their solubility.
2. Disruption of the primary solvent structure. In aqueous systems the hydrogen bonding network of water generates a structured solvent environment which often

disfavors solvation of hydrophobic solute. A cosolvent can disrupt (or weaken) that network, thus reducing the entropic and enthalpic penalty for dissolving hydrophobic species.

3. Alteration of solute–solvent and solute–cosolvent interactions. The presence of cosolvent can modify the local composition surrounding a solute molecule, leading to preferential solvation by organic-solvent molecules or mixed solvent shells. This change in local environment mitigates the unfavorable interactions encountered in pure water.

While cosolvency is a practical and widely used strategy, several considerations must be taken into account. Upon dilution with water, the solvent composition may shift away from the solubilizing region, leading to solute precipitation. In surfactant-based formulations, the addition of cosolvent alters the solvent polarity and reduces the solvophobic driving forces responsible for micellization and adsorption, processes that are essential for cleaning performance. As a result, while solubility may improve, the overall efficiency of soil removal can be compromised. Furthermore, the relationship between solubility and cosolvent concentration is not always linear;[27,28] beyond a certain concentration, solubility gains often diminish or reach a maximum. In some solvent systems, a decrease in solubility can even occur with increasing cosolvent fraction, a phenomenon known as cononsolvency, which must be evaluated on a case-by-case basis.

Hydrotropes

Hydrotropy, first defined in the early 20th century by Neuberg,[29] refers to the notable increase in the water solubility of hydrophobic compounds when specific water-soluble organic compounds, known as hydrotropes, are introduced. Hydrotropes possess both hydrophilic and hydrophobic regions. Structurally, hydrotropes are diverse, comprising both ionic and nonionic species. Their hydrophobic part can range from short alkyl chains

to aromatic rings. While hydrotropes share some similarities with surfactants, such as their amphiphilic nature, they differ in their limited ability to self-assemble and their minimal effect on reducing surface tension. This distinction arises because their hydrophobic portions are typically too small to induce micelle formation.

In industry, hydrotropes are valued for their versatility. They have been used in a range of areas, including cosmetics, pharmaceuticals, and processes such as separation, solubilization, and extraction. They are also common additives in detergents, surfactants, and polymer formulations. Despite their long history and widespread use, the precise mechanisms by which hydrotropes enhance solubility remain a topic of debate. Several explanations have been proposed:[30]

1. Complex formation between hydrotrope molecules and solutes.
2. Disruption of the solvent structure; hydrotropes can interfere with the hydrogen-bonded network of the water, a process similar to that observed with cosolvents.
3. Self-association, the most widely supported hypothesis; it supports that hydrotropes self-associate with the substance to solubilize above a critical aggregation concentration, forming aggregates that behave similarly to micelles.

In surfactant solutions, hydrotropes play a vital role by preventing phase separation, which can otherwise limit the solubilization capacity. The way hydrotropes work in these systems involves forming mixed micelles composed of both hydrotrope and surfactant molecules. Because of their relatively large hydrophilic heads and small hydrophobic groups, hydrotropes tend to form spheroidal structures rather than lamellar or liquid crystalline ones. This change in aggregate shape modifies the natural association patterns seen in pure surfactant solutions. Hydrotropic action, therefore, occurs at concentrations where hydrotropes start to self-associate and form these mixed structures with surfactants.[31]

Unlike the well-established behavior of classical surfactants, hydrotropes continue to generate discussion in scientific literature.[24,30,32–34]

Hydrotropes thus offer a distinctive advantage over cosolvents in surfactant-based formulations. While both approaches enhance solubility by modifying the local solvent environment, hydrotropes do so without fully suppressing the solvophobic interactions that drive micellization and adsorption. Instead, by forming mixed aggregates with surfactants, hydrotropes preserve or even enhance these processes, maintaining cleaning efficacy while improving phase stability. In contrast, cosolvents tend to weaken hydrophobic interactions more uniformly throughout the medium, which can reduce micellar formation and, consequently, the efficiency of surfactant-driven cleaning mechanisms.

Secondary Surfactants

Beyond cosolvents and hydrotropes, secondary surfactants represent a third class of solubilizing agents that are themselves amphiphilic and capable of self-assembly. They are often incorporated to improve the solubility of highly hydrophobic surfactants in water, forming mixed surfactant systems. In these systems, cooperative self-association driven by the hydrophobic effect gives rise to synergistic behavior, where aggregates composed of different surfactant types exhibit lower critical micelle concentrations (CMC) and interfacial tensions than would be expected from the pure components. When mixtures include surfactants of different ionic character, electrostatic interactions between head groups can further promote association at lower concentrations. Ideally, the formation of randomly mixed aggregates is favored, as the hydrophobic effect is largely independent of the specific nature of the polar head group.

The observed synergism arises primarily from non-ideal mixing effects within the aggregates. As a result, the tendency to form aggregates in surfactant mixtures can differ markedly from that in pure surfactant solutions. A key implication of non-ideal mixing is

that the composition at the interface or within micelles can deviate significantly from that of the unassociated surfactant molecules in bulk solution. This distinction is important because interfacial adsorption involves only unimers, monomeric surfactant molecules in the bulk solution, while the solubilization of hydrophobic compounds occurs within micelles. Typically, the most surface-active components preferentially occupy interfaces and micelles, whereas more water-soluble components remain enriched in the bulk phase.

Secondary surfactants are often chosen as solubilizers over cheaper hydrotropes due to their multifunctional benefits in cleaning formulations. Unlike hydrotropes, secondary surfactants actively migrate to surfaces, directly aiding in cleaning. They provide high solubilization of hydrophobic surfactants at relatively low concentrations and contribute to foam control, viscosity adjustment, and formulation stability in alkaline or electrolyte-rich environments. Additionally, they help maintain the homogeneity of formulations by solubilizing components such as solvents, perfumes, and dyes.

2.3.2 Chelating Agents

Chelating agents are molecules that attach to metal ions through two or more electron donor atoms, forming ring structures, a process known as chelation. These agents play a critical role in cleaning formulations by addressing a major challenge: water hardness.

In hard water, the presence of metal ions like calcium, magnesium, and iron can bind to surfactants, especially anionic surfactants, rendering them less effective or even causing them to precipitate. This in turn can reduce or fully deplete a detergent of its cleaning capability. Chelating agents prevent this by binding to the metal ions, preventing them from interfering with the surfactant molecules.

Beyond their role as water softeners, chelating agents play a critical role in cleaning. Their ability to bind and sequester metal ions directly contributes to the removal of challenging soils. For example, in the removal of limescale, primarily composed of calcium and

magnesium carbonates, chelating agents solubilize these metal ions, allowing the scale to be lifted from surfaces without the need for harsh acidic cleaning agents.

In addition to removing scale, chelating agents are effective in breaking down soils stabilized by metal ions, such as dairy residues that contain calcium. By binding to the metal ions within the soil matrix, the chelating agent weakens the attachment of the soil to surfaces. Chelating agents are also highly effective at treating metal oxide-based stains, such as rust.

Furthermore, most chelating agents provide a beneficial buffering effect, helping to maintain an alkaline pH. As discussed earlier, an alkaline pH deprotonates acidic soils and creates negative charges on both the soil and the substrate. This leads to the formation of a diffuse layer of counterions between them, which promotes an osmotic flow of water into the area, lifting the soil.

Chelating agents can generally be classified as (i) hard chelating agents which would be those of the aminopolycarboxilic types, citric acid and sodium gluconate and (ii) soft ones which would be mostly of polymeric nature such as sodium polyacrylate. The former binds strongly to metal ions with one chelating agent binding to one cation, the latter binds more loosely and the stoichiometry (ratio) of binding is variable. The focus in this thesis is on hard chelating agents.

Aminopolycarboxylates are prominent metal chelators, with nitrilotriacetic acid being the first commercially produced in 1936, followed by ethylenediaminetetraacetic acid (EDTA) in 1939. These chelating agents gained widespread use after 1967, when tripolyphosphates were banned in several countries. However, concerns over their ecological impact, toxicity, and poor biodegradability led to the search for more environmentally friendly alternatives. In the 1990s, methylglycinediacetic acid (MGDA) and tetrasodium glutamate diacetate (GLDA) emerged as popular replacements in several applications.

A common issue in formulations containing nonionic and/or ionic surfactants is the salting-out effect caused by chelating agents, which leads to micellar growth and precipitation. This effect is attributed to the strong hydration and water-structuring properties of the chelating agents. Beyond the salting-out effect, the detailed interactions between chelating agents and surfactants have been minimally explored. The existing literature can be divided into two main areas: studies on traditional chelating agents, such as EDTA, and research focused on practical applications, which often lack a comprehensive investigation into the chemical mechanisms driving these processes.

For example, Zhao *et al.*[35] studied the impact of EDTA on gemini cationic surfactants and found that the interaction led to the formation of oligomeric surfactant analogues, which self-assemble at lower concentrations than the CMC of the pure surfactant. This self-assembly is attributed to electrostatic binding between the carboxylate groups of EDTA and the ammonium group of the surfactant. Similarly, Soontravanich *et al.*[36] observed a synergistic effect on soap scum solubility at high pH when using a mixture of amine oxide-based surfactants and EDTA. The solubility was found to be significantly higher compared to chelate-free systems, likely due to the formation of mixed micelles between stearate anions and the surfactant, promoted by EDTA and chelated Ca^{2+} ions.

Yunusov *et al.*[37] used molecular simulations to investigate surfactant-EDTA systems and found that EDTA disrupts hydrogen bonding between water molecules and between water and surfactants, suggesting its role as a salting-out agent. This disruption reduces surfactant hydration and increases monolayer packing due to electrostatic repulsion. Additionally, their results showed that EDTA accumulates at the interface, thickening the interfacial layer, a trend also observed in systems containing both surfactant and chelating agent.

Studies on the interactions between amino acids and surfactants offer valuable insights into the effects of chelating agents on surfactant self-assembly. Yan *et al.*[38] found that, similar to

the EDTA-surfactant system, the CMC of cationic surfactants decreases in the presence of amino acids, but also the aggregation number decreases, suggesting that these small molecules promote micelle formation. Chauhan and Sharma[39] proposed that amino acids could influence the hydration shell around the alkyl chain of the surfactant by interacting with its head group. Likewise, Kandpal *et al.*[40] observed that in systems with anionic surfactants and glycine, this interaction occurs at low surfactant concentrations, reaching a saturation point. Additional surfactant causes a regular micellization process in the presence of additives. Such interactions are well-documented, with most studies highlighting the coexistence of a surfactant with an ammonium-based head group and an amino acid in aqueous solution.[41–43]

Most of the literature on GLDA and MGDA tends to focus on practical applications, such as enhanced oil recovery in oil fields[44,45] and cloud point extraction in water treatment.[46] These studies typically focus on performance metrics like recovery rates and surface tension variations under different experimental conditions, leaving a noticeable lack of molecular-level investigations into these systems. To address this gap, the present work explores the interactions between amine-based surfactants and chelating agents, hypothesizing that these interactions can help prevent salting-out effects and even promote the solubilization of hydrophobic nonionic surfactants. This ability to solubilize hydrophobic surfactants is especially relevant in highly concentrated systems, such as those used in various industrial applications like cleaning, agriculture, and oil field processes.

2.3.3 Amphoteric Surfactant–Chelating Agent Systems

Beyond their individual roles in formulations, surfactants and chelating agents can display synergistic behavior when combined. Amphoteric surfactants, in particular, have been reported to form unusually stable mixtures with chelating agents such as glutamic acid diacetate (GLDA)[47] Early screening studies showed that while many nonionic, anionic, or

cationic surfactants phase-separated or caused turbidity when added at high concentration to aqueous GLDA solutions, amphoteric surfactants maintained clarity and acceptable viscosity even at high mixing ratios. In some cases, formulations with a 1:1 weight ratio of GLDA to amphoteric surfactant remained stable, an outcome not readily predicted from their individual properties. These clear and stable solutions also allowed the incorporation of additional surfactants and polymers without compromising formulation stability.

Further observations revealed non-classical effects on solubility and cloud point behavior in systems containing poorly soluble nonionic ethoxylated surfactants. For instance, in systems with both nonionic and amphoteric surfactants, the addition of GLDA could either increase or decrease the cloud point depending on the mixing ratio. Such effects suggest that amphoteric surfactant–chelating agent interactions involve specific molecular associations that modify micellar or aggregate structures in ways not captured by conventional models of surfactant solubility and additive effects.

These peculiar behaviors provide a strong rationale for investigating amphoteric surfactant–chelating agent systems in greater detail. By linking empirical formulation stability to fundamental physicochemical interactions, they offer an opportunity to extend classical understanding of micellization and solubilization into multicomponent systems relevant for concentrated cleaning products.

CHAPTER 3

Experimental methodology

3.1. Materials

All surfactants used in this study were technical-grade products and were employed without further purification. As a result, the materials consist of complex mixtures containing unreacted starting materials, side products, and a range of closely related chemical structures. For ethoxylated nonionic surfactants, the reported degree of ethoxylation corresponds to an average value over a distribution of oligomer lengths. For the amphoteric surfactants, the reported degree of nitrogen substitution represents the maximum achievable substitution, while an estimated 30 percent of the molecules remain partially substituted. These characteristics reflect the inherent heterogeneity of industrial surfactants and are considered representative of surfactant formulations used in practical applications.

The chelating agents employed in this work were technical-grade materials and were used as received. According to supplier information, these products contain residual sodium hydroxide and are supplied as alkaline solutions with a typical pH value of

approximately 11.5. In contrast, the surfactant materials are reported to exhibit neutral to mildly basic pH values, generally below 9. The pH of the prepared samples was routinely measured and was left unadjusted unless explicitly stated in the corresponding experimental data.

3.2. NMR to Explore Molecular Interactions in Surfactant Systems

3.2.1 Instrumentation

NMR experiments were performed using a 400 MHz Varian VNMRS spectrometer equipped with a broadband probe suitable for both ^{1}H and ^{13}C detection, with temperature control provided by the spectrometer unit. The instrument was located at the Innovation Center of Nouryon in Stenungsund, Sweden. A sealed glass capillary containing deuterated methanol was placed inside the sample tubes to provide a lock signal and reference for ^{13}C measurements, without introducing solvent into the sample and avoiding potential interference with micellar organization. Detailed experimental parameters and acquisition protocols for the individual NMR experiments are reported in the corresponding publications included in this thesis.

3.2.2 Fundamental Principles of NMR Spectroscopy

Nuclear Magnetic Resonance (NMR) spectroscopy operates on the principle that certain atomic nuclei, when placed in a strong magnetic field, will respond to radiofrequency radiation by emitting signals. These signals are highly characteristic of the nuclei and depend on factors such as the strength of the magnetic field, the chemical environment, and the specific magnetic properties of the isotope being studied. Nuclei such as hydrogen (^{1}H) and carbon-13 (^{13}C), possess a non-zero spin, which gives them a magnetic moment and angular momentum, making them detectable by NMR.

In a typical NMR experiment, nuclear spins are first partially aligned by a strong, constant magnetic field (B_0). A radiofrequency (RF) pulse is then applied to perturb this alignment, tipping the net magnetization away from equilibrium and causing it to precess at the Larmor frequency, which is determined by the gyromagnetic ratio of the nucleus and the strength of the applied magnetic field. This frequency difference, recorded as the chemical shift, varies according to the chemical environment of each nucleus, allowing NMR to differentiate between distinct molecular environments.

The unique strength of NMR spectroscopy lies in its ability to provide detailed insights into molecular structure and dynamics by detecting subtle interactions between nuclear spins and their surrounding environments. More importantly, NMR can independently observe each component in a complex mixture, allowing for an in-depth study of how individual surfactant molecules and other formulation ingredients behave and interact within the mixture. Rather than focusing on the technical aspects of each NMR method, this section highlights the types of insights that NMR studies can offer for surfactant systems.

To complement the conceptual overview presented in the following subsections, Figure 6 illustrates the spectral features evaluated throughout this study: the chemical shift, and the line width at half-maximum intensity (FWHM), serving as a reference for the analytical approaches described in Sections 3.2.3 and 3.2.4.

3.2.3 Chemical Shift Variations

Chemical shifts in NMR spectroscopy reveal valuable information about the electronic environment surrounding a nucleus, and by extension, the molecular environment of surfactants as they interact and aggregate. When surfactants begin to form micelles, changes in their chemical environment leads to observable changes of their NMR spectra.[48] This transformation, from individual molecules dissolved in solution to those aggregated within micelles, can be tracked by monitoring the changes in chemical shift.

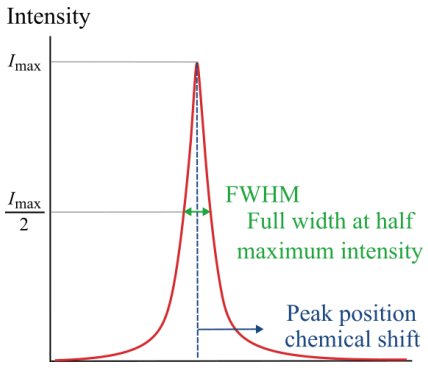

Figure 6. Schematic overview of chemical shift and signal broadening in a representative NMR peak. The chemical shift is a proxi for the electronic environment of a nuclei, while the signal width at half-maximum intensity can reflect dynamic processes such as molecular exchange, aggregation, or binding events.

Below the CMC, the surfactant molecules primarily exist as isolated units, or unimers, within an aqueous environment, generating characteristic chemical shifts typical of this state. As the concentration reaches the CMC, the hydrophobic tails of the surfactants begin to aggregate, moving into the micellar core, an aliphatic environment. This change in environment leads to a distinct change in the observed chemical shift,[49] δ_{obs}, which reflects a population average between micellized (δ_m) and unimeric (δ_u) states:

$$\delta_{obs} = \delta_u \left(\frac{C_u}{C_T}\right) + \delta_m \left(\frac{C_m}{C_T}\right) \quad (2)$$

here, C_u and C_m are the free surfactant concentration and the concentration of surfactant in the micelles, respectively; and $C_T = C_u + C_m$ is the total surfactant concentration. By plotting chemical shift variations as a function of surfactant concentration, the CMC can be determined and the aggregation number estimated.[50,51]

Similarly, dynamic molecular equilibria, such as binding interactions between two different molecules, alter the chemical environment of the atoms involved in the interaction. The fast exchange kinetics between bound and unbound states, relative to the time scale of NMR detection, leads to the observation of a

population-weighted average chemical shift. In formulations where surfactants interact with secondary ingredients, the observed chemical shift reflects contributions from surfactants in multiple states: as unimers, as part of micelles, and as surfactants interacting with secondary ingredients either in unimeric form or within micellar structures.

3.2.4 Analysis of Spectral Line Shape

Chemical exchange, a dynamic process where molecules transition between different states, such as free and bound forms, not only generates chemical shift variations in NMR spectra, but also influences the shapes of the NMR signals. The line shape is a direct result of the time-dependent magnetic environments change which disrupts phase coherence. In a two-state system, where a molecule M binds to a ligand L to form a complex ML, the exchange rate k_{ex} is given by:

$$k_{ex} = k_{on}[L] + k_{off} \tag{3}$$

The appearance of an NMR signal depends on the relationship between the exchange rate k_{ex} and the frequency difference $\Delta\omega$ between the free and bound states.[52,53] In the fast exchange regime ($k_{ex} \gg \Delta\omega$), a single resonance appears at a chemical shift that represents a population-weighted average of the two states. In the slow exchange regime ($k_{ex} \ll \Delta\omega$), two distinct signals appear, representing the chemical shifts of the free and bound states, each weighted by their respective populations. When the exchange rate is intermediate ($k_{ex} \approx \Delta\omega$), extensive line broadening occurs, reflecting the fluctuations between states at the time scale of the frequency difference.

This sensitivity to exchange kinetics, along with factors such as state population and chemical shift differences, makes line shape analysis a powerful tool for characterizing molecular equilibria and binding interactions. By examining changes in line shapes under various conditions, the strength and dynamics of interactions between surfactant

molecules, or between surfactants and other components in a mixture, can be effectively assessed.

3.2.5 Advantages and Limitations of ^{13}C NMR in Surfactant Analysis

While ^{1}H NMR remains the most commonly used technique in surfactant research,[61–65] ^{13}C NMR offers complementary insights by directly probing the carbon backbone of surfactant molecules.[50,66,67] A key advantage of ^{13}C NMR lies in the generation of separate signals for each carbon atom, including quaternary carbons that are invisible to ^{1}H NMR. This makes ^{13}C NMR particularly valuable for characterizing complex surfactants and for detecting nonuniform changes across the molecule.

As a case in point, sodium octanoate exhibits eight well-resolved ^{13}C signals corresponding to its eight carbon atoms.[51,68] The corresponding ^{1}H NMR spectrum, however, reflects the equivalence of many protons along the lipophilic chain, resulting in only a few distinct resonances. Figure 7 compares the ^{1}H and ^{13}C spectra of one surfactant used in this study, highlighting how ^{13}C NMR enables a more detailed characterization of the lipophilic chain. In the ^{1}H spectra, two signals represent six different proton environments, whereas in the ^{13}C spectra, each carbon nucleus along the lipophilic chain is resolved into an individual peak.

Additionally, ^{13}C NMR offers a broader chemical shift range,[50,51] attributed to the strong sensitivity of carbon shielding to bonding, hybridization, and the local electronic structure. This wider range brings two key advantages.

First, it reduces spectral overlap, enabling individual assignment of peaks corresponding to different molecules, which is particularly valuable in formulations containing multiple ingredients. Figure 7 illustrates this in two ways: (i) through the greater number of

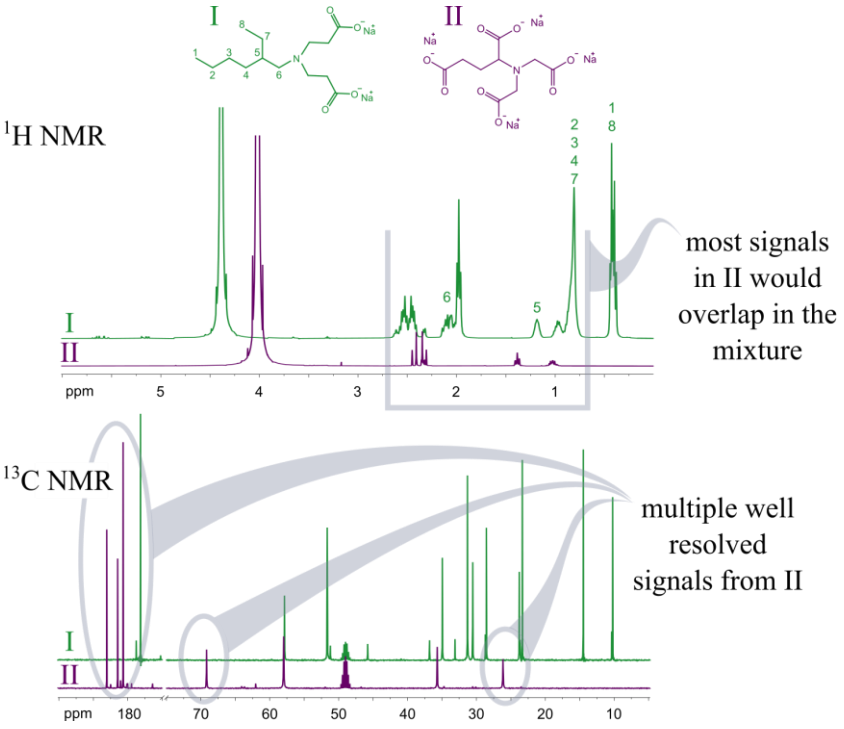

Figure 7. Comparison of ^{1}H and ^{13}C NMR spectral resolution. Top: surfactant (I, green) and chelating agent (II, purple), with the surfactant lipophilic chain numbered. Middle: stacked ^{1}H spectra, where equivalent protons in the surfactant chain collapse into two signals, with additional overlap expected from the chelating agent in a mixture. Bottom: stacked ^{13}C spectra, where all carbons of the surfactant chain are individually resolved and the chelating agent peaks remain separated, illustrating the improved assignment and reduced overlap offered by ^{13}C NMR.

distinguishable signals along the surfactant tail, as noted above, and (ii) by comparing the ^{1}H and ^{13}C spectra of the two individual components in a representative system, where ^{13}C NMR would preserve greater signal separation in the mixture, whereas ^{1}H NMR signals would overlap.

Second, the broader chemical shift range enhances the detection of structural changes, such as micellization. This benefit has been demonstrated in studies using ^{19}F NMR for fluorosurfactants,[69–71] where the extended chemical shift range reveals finer details on the molecular reorganization.

However, ^{13}C NMR has certain limitations. ^{13}C has a much lower natural abundance which gives a much lower sensitivity compared to ^{1}H NMR, requiring higher sample concentrations or extended acquisition times to achieve

sufficient signal strength. This drawback can make ^{13}C NMR less practical for rapid or low-concentration measurements. Despite these limitations, ^{13}C NMR remains a valuable tool for studying surfactant systems, offering complementary information that enhances our understanding of complex formulations, particularly when multiple surfactants or additives are involved.

3.2.6 Diffusion NMR

Diffusion NMR, also known as Diffusion Ordered SpectroscopY (DOSY), NMR diffusometry or pulsed field gradient NMR, is a powerful technique used to measure self-diffusion coefficients of molecules in solution.[54–59] This method combines RF pulses with pulsed field gradients to analyze molecular movement, providing critical information about molecular size, shape, and interactions in complex chemical systems.[60]

The fundamental pulse sequence in diffusion NMR is the pulsed field gradient spin-echo (PGSE) sequence. In this approach, magnetization is first excited by a 90-degree RF pulse, followed by a magnetic field gradient pulse that phase encodes the magnetization. It means that the spatial location of molecules is encoded before a delay, denoted diffusion time. After half of the diffusion time, a 180-degree RF pulse inverts the magnetization, and a second gradient pulse is applied to refocus the signal. Only spins belonging to molecules that have remained in the same location during the diffusion time will refocus completely, while those that have diffused reduce the intensity of the NMR signal. This attenuation of the signal is related to the self-diffusion coefficient, strength and duration of the gradient pulse, as well as the diffusion time.

In a diffusion NMR experiment, the gradient strength is incrementally increased while all other parameters are held constant. The attenuation of the normalized signal is described by the Stejskal–Tanner equation,

$$\left(\frac{S_{(2\tau)}}{S_{(0)}}\right) = e^{\left[-D\gamma^2G^2\delta^2\left(\Delta-\frac{\delta}{3}\right)\right]} \tag{4}$$

where γ is the gyromagnetic ratio, G the gradient strength, δ the gradient duration, and Δ the diffusion time, whose combined term defines the k value. For illustration, the Stejskal–Tanner expression may be written in its linearized form,

$$\ln\left(\frac{S_{(2\tau)}}{S_{(0)}}\right) = -Dg^2G^2\delta^2(\Delta - {}^{\delta}/_{3}) \tag{5}$$

for which unrestricted diffusion corresponds to a linear dependence on the diffusion weighting factor. However, the determination of the self-diffusion coefficient is carried out by fitting the untransformed monoexponential decay of the normalized signal as a function of the k value, preserving the physical form of the Stejskal–Tanner relationship and providing an accurate extraction of D.

In systems undergoing chemical exchange, the appearance of the decay depends on the exchange regime. For fast exchange, where interconversion between species occurs more rapidly than the diffusion timescale, the experiment yields a single monoexponential decay corresponding to a population-weighted diffusion coefficient. When exchange is slow, the signal instead displays a multiexponential decay, with each exponential term representing the self-diffusion coefficient of a distinct, non-interconverting species.

The extracted diffusion coefficients can be related to hydrodynamic size through the Stokes-Einstein equation:

$$D = \frac{\mathrm{k}T}{6\pi\eta r} \tag{6}$$

where k is the Boltzmann constant, T is the temperature, η is the viscosity of the solvent, and r is the radius of the molecule. This relationship shows that larger or more highly associated species diffuse more slowly, and that diffusion increases in less viscous solvents.

Diffusion NMR has diverse applications, including tracking molecular interactions and exchange, calculating association constants, studying encapsulation and molecular cages, and analyzing ion pairing and organometallic systems. It also provides information on molecular size and shape for small molecules, complexes, dendrimers, and polymers, making it invaluable for characterizing multicomponent systems.

3.3. Dynamic Light Scattering (DLS)

DLS is a widely used technique for probing the size and dynamic behavior of colloidal particles and molecular aggregates in solution.[72,73] A coherent laser beam illuminates the sample, and particles undergoing Brownian motion scatter the incident light. Because the laser light is coherent, the relative phases of the scattered wavelets at the detector are determined by the instantaneous positions of the diffusing particles. The detector receives the sum of these wavelets at each moment, and their superposition forms the instantaneous electric field $E(t)$. At a slightly later time t + τ, the particles have moved to new positions due to diffusion, resulting in a modified superposition and a new electric field $E(t + \tau)$. As this process continues, the detected electric field fluctuates in time, and its fluctuation rate reflects the translational diffusion of the scattering species.

These electric field fluctuations are analyzed through the temporal autocorrelation function of the scattered intensity. The decay rate of the autocorrelation function is directly related to the translational diffusion coefficient of the particles. Using the Stokes–Einstein relationship, eq. (6), the diffusion coefficient can then be converted into a hydrodynamic radius, which represents the effective size of the diffusing species in solution.

In surfactant systems, DLS provides valuable information about micellar size, aggregation number, and changes in hydrodynamic radius upon variations in composition, concentration, temperature, or the presence of additives such as salts, polymers, or chelating agents. Although DLS does not directly distinguish between different aggregate shapes, variations in the apparent diffusion coefficient or in sample polydispersity often reflect structural transitions, such as the formation of elongated micelles. Because the scattered intensity scales with the sixth power of particle size, DLS is particularly sensitive to the presence of larger aggregates, making it an effective technique for detecting the onset of micellar growth or phase separation.

DLS experiments were carried out using an Anton Paar Litesizer 500 equipped with a 658 nm laser, located at Chalmers University of Technology in Gothenburg, Sweden. Measurements were performed under standard conditions at 25 °C using a 90° detection angle. Detailed measurement parameters and data processing procedures are reported in the corresponding publications included in this thesis.

In this work, DLS measurements were used to evaluate how chelating agents influence micellar size and dynamics in mixed surfactant systems. The measured hydrodynamic diameter served as an indicator of changes in aggregate size and was interpreted in conjunction with cloud point and diffusion NMR data to identify differences in micellar association and molecular mobility.

3.4. Small-Angle Neutron Scattering (SANS)

SANS is a structural characterization technique that probes the size, shape, and internal organization of colloidal and self-assembled systems on length scales from approximately 1 to 200 nm.[74] A monochromatic neutron beam is directed through the sample, and neutrons are elastically scattered by spatial variations in scattering length density. These variations

arise from differences in nuclear scattering properties between regions of the material, such as the contrast between the hydrophobic core and hydrophilic shell of a micelle, or between solvent and solute. At the detector, the scattered neutrons are recorded as a function of the scattering vector q, which is related to the scattering angle and neutron wavelength. The resulting intensity profile $I(q)$ encodes information on characteristic distances, particle dimensions, and spatial correlations within the system.

The underlying contrast mechanism in SANS is based on coherent scattering from atomic nuclei, which gives the technique a unique sensitivity to light elements and isotopes. In particular, the strong difference in scattering length between hydrogen and deuterium enables fine control of scattering contrast through selective deuteration or solvent contrast variation. By adjusting the relative scattering contributions of different components, SANS can highlight or suppress specific regions of a self-assembled structure, isolate one component in a multicomponent mixture, or distinguish between coexisting micellar populations. This tunable contrast capability is one of the defining strengths of neutron scattering, as it enables selective visualization of different components within complex assemblies.

In surfactant solutions, the analysis of $I(q)$ allows determination of micellar size, shape, aggregation number, and internal organization. The form of the scattering curve reflects the overall particle geometry:[75] spherical micelles produce characteristic Guinier and Porod regimes, while ellipsoidal, cylindrical, or wormlike micelles exhibit distinct signatures in the q-dependence of the intensity. Through model-based fitting of the scattering profile, parameters such as core radius, shell thickness, micellar length, and persistence length can be quantified. In addition, changes in these parameters with composition, temperature, or the presence of additives provide insight into structural transitions, micellar growth, and the emergence of anisotropic aggregates.

SANS measurements were performed on the SAM instrument at the Institut Laue–Langevin in France. The instrument covered a broad range of scattering vectors, enabling characterization of micellar structures across multiple length scales. Detailed measurement parameters, sample preparation, and data analysis procedures are reported in the corresponding publications included in this thesis.

3.5. Surfactant Formulations: Key Properties for Cleaning

Designing an effective test for evaluating the functional performance of a surfactant formulation is often challenging, as no single laboratory test can replicate the wide range of real-world conditions and applications.[2] While specific tests exist for properties such as detergency, wetting, lubrication, defoaming, and dispersion, they cannot individually address the diverse needs of end-users. Therefore, it is more practical to begin with quick, simple, and cost-effective tests to screen potential surfactants or formulations.

Basic tests measuring parameters such as viscosity, cloud point, surface tension, and contact angle on hydrophobic surfaces can be conducted efficiently and provide key insights into the physicochemical behavior of a formulation.

To complement these physicochemical characterizations, two functional tests were included to assess cleaning-related performance: a non-mechanical cleaning test and an oil incorporation capacity test. These methods represent two distinct ends of the cleaning spectrum. The non-mechanical cleaning test mimics low-energy, short-contact-time applications in which wetting and rapid soil detachment dominate performance, typical of hard-surface cleaning. The oil incorporation capacity test reflects a different cleaning regime, characteristic of high-energy cleaning scenarios, such as laundry, where mechanical input is substantial, and performance relies primarily on solubilization, emulsification, and dispersion of hydrophobic soils. Together, these tests provide a more complete view of how

surfactant formulations behave under conditions relevant to practical cleaning applications and offer a functional complement to the physicochemical measurements used in this work.

The experimental procedures associated with these physicochemical and functional tests are presented in the accompanying articles, and their theoretical foundations have been discussed in Chapter 2. The next section addresses the outstanding topic: how viscosity, micellar structure, and surfactant solution behavior relate to cleaning performance.

3.5.1 Viscosity

Viscosity describes the resistance of a fluid to flow and reflects how strongly its molecules interact as they pass one another. In this sense, viscosity can be understood as a form of molecular friction: the stronger the interactions within the fluid, the more energy is required to make it flow.

In surfactant solutions, viscosity is closely linked to micellar structure and how it evolves with concentration and formulation conditions.[76] Just above the critical micelle concentration (CMC), micelles are typically small and spherical, the simplest and most symmetric morphology. As concentration increases, micellar growth can occur, leading to changes in size, shape, and aggregation number. For short-chain surfactants such as C8 or C10, micelles tend to remain small and spherical even at relatively high concentrations (up to 40 wt%), resulting in only gradual increases in viscosity, as expected for dispersions of roughly spherical particles.[4] As the hydrophobic chain length increases (C14 and above), micelles more readily elongate and may evolve into rod-like or thread-like structures at higher concentrations. These anisotropic micelles have larger surface areas and a greater tendency to interact or entangle, both of which contribute to pronounced increases in viscosity. Such structural transitions are influenced not only by surfactant type and concentration but also by temperature, electrolyte content, and other physicochemical parameters that affect micellar stability and packing. In this thesis, changes in viscosity are

associated with these structural transitions and correlated to intermolecular interactions taking place in surfactant systems.

In addition to the microscopic changes, understanding and managing viscosity is essential in the design of cleaning formulations for technical, safety, and marketing purposes. From a technical standpoint, increased viscosity can improve surface adhesion, promote uniform coverage, and enhance contact time, which is especially beneficial for applications on vertical surfaces. Moderate viscosity also contributes to the stability of dispersed phases, helping maintain the integrity of active ingredients and prolong shelf life. An optimized viscosity profile is therefore necessary: it allows the product to flow and be dispensed easily, while simultaneously providing sufficient structural resistance to maintain stability during storage. From a safety perspective, a thicker consistency can reduce the risk of spills or splashes, particularly when formulations contain potentially harmful or irritant ingredients. Finally, consumer perception also plays a role, as end users often associate higher viscosity with greater product quality and effectiveness.

CHAPTER 4

Results and Discussion

The ternary systems discussed in this section consist of amphoteric and nonionic surfactants combined with chelating agents. Throughout this section, the terms binary and ternary systems refer exclusively to the number of surfactant and chelating agent components present in the formulation, with water treated as the solvent and not counted as a component. Accordingly, ternary systems comprise an amphoteric surfactant, a nonionic surfactant, and a chelating agent dissolved in water, whereas binary systems comprise an amphoteric surfactant and a chelating agent dissolved in water.

Two amphoteric surfactants were studied: a branched variant (BC8Amph) and a linear variant (LC12Amph). Both were combined with a poorly water-soluble linear nonionic surfactant (LC10 4EO) and either GLDA or MGDA as the chelating agent. Chemical structures, full names, and abbreviations for these compounds are summarized in Figure 8.

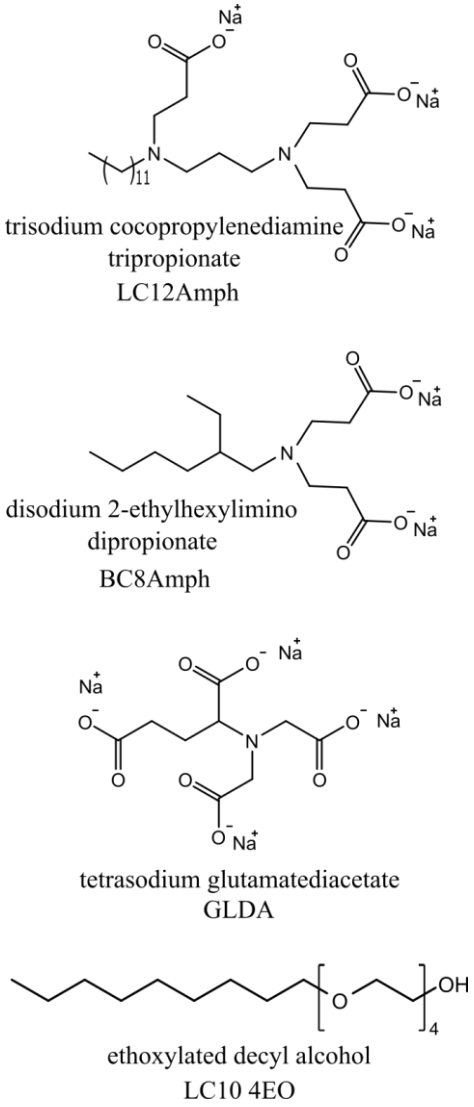

Figure 8. Chemical structures of the chelating agents and surfactants evaluated. The abbreviated names used are included for clarity.

4.1. The Role of pH and Specific Interactions in Surfactant–Chelating Agent Systems

Before addressing the molecular interactions in surfactant–chelating agent systems, it is important to consider the role of pH. Amphoteric surfactants are sensitive to pH, as changes in protonation state alter their charge characteristics. For the surfactants considered here, the pKa of the nitrogen-containing groups is typically in the range of pH 9–10. At pH values below this range, the amine groups are predominantly protonated, whereas at higher pH they become deprotonated, increasing the net negative charge on the surfactant and modifying headgroup interactions. In micellar systems, this pH sensitivity is further amplified because the apparent pKa depends strongly on the self-assembled state of the surfactant and is often shifted to higher values compared to the unimeric form.[77–79]

Chelating agents such as GLDA and MGDA, which are inherently alkaline, increase the pH of the solution when added, thereby altering the protonation state of the amphoteric surfactant. This

effect alone can produce nonmonotonic changes in cloud point values. As the surfactant passes through its isoelectric point, initial deprotonation increases solubility and headgroup repulsion, resulting in smaller micelles and higher cloud points. At higher chelating agent concentrations, the inherent salting-out effect of the chelating agent eventually counterbalances the pH-driven solubilization, causing the cloud point to decrease. Figure 9 compares the cloud point of amphoteric/nonionic surfactant systems with and without chelating agents as a function of pH.

The comparison highlights that the non-monotonic behavior of cloud points is influenced by pH changes, as the protonation state of the amphoteric surfactant passes through its isoelectric point. However, the higher cloud points observed in the presence of chelating agents, even at equivalent pH, indicate that pH alone does not fully explain the behavior of the system. While cloud point measurements reflect the combined effects of pH and the surfactant–chelating agent interactions, diffusion NMR provides a means

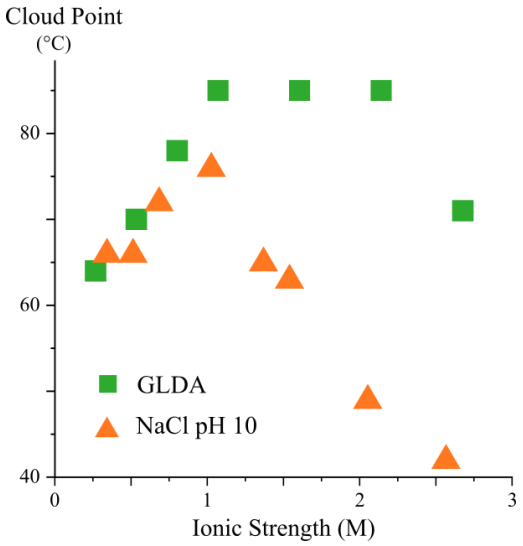

Figure 9. Cloud point changes for mixtures of nonionic and branched amphoteric surfactants upon addition of GLDA (squares) or NaCl at pH ≥ 10 (triangles).

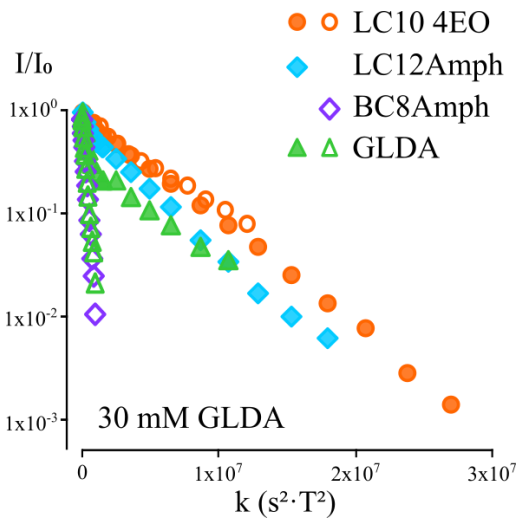

Figure 10. Stejskal–Tanner plots for ternary mixtures of nonionic surfactant, amphoteric surfactant, and GLDA. Filled symbols denote systems with the linear amphoteric; unfilled symbols denote systems with the branched amphoteric. Circles, diamonds, and triangles represent the nonionic surfactant, amphoteric surfactant, and GLDA, respectively.

to distinguish between these contributions by probing the mobility of individual components (Figure 10). For the same ternary systems, the diffusion behavior of the chelating agent closely follows that of the amphoteric surfactant. When the amphoteric surfactant remains largely in the bulk solution, as observed with the branched variant, the chelating agent also diffuses rapidly. In this case, the similar diffusion rates can be rationalized by the comparable hydrodynamic sizes of GLDA (351 g/mol) and the branched amphoteric surfactant (317 g/mol).

However, when the amphoteric surfactant partitions into micelles, as seen for the linear variant, the diffusion of the chelating agent decreases and matches the micellar motion. While protonation of GLDA at low concentrations may influence its physicochemical properties, the observed diffusion behavior cannot be fully rationalized by pH effects alone. The results instead indicate that the chelating agent is associated with the micellar structures, leading to diffusion characteristics coupled to those of the amphoteric surfactant. This provides strong evidence in favor of specific molecular interactions within the system.

4.2. General Features of Surfactant–Chelating Agent Associations

The fundamental features of the association between amphoteric surfactants and chelating agents were examined using binary systems containing amphoteric surfactant and chelating agent, without any nonionic surfactant present. Carbon-13 NMR spectroscopy was used to evaluate whether the two components interact in solution. The analysis relied on comparing spectra collected at increasing surfactant concentrations while keeping the chelating agent concentration constant. Systematic changes in chemical shift and line broadening were used as indicators of molecular association. A representative example is shown in Figure 11,

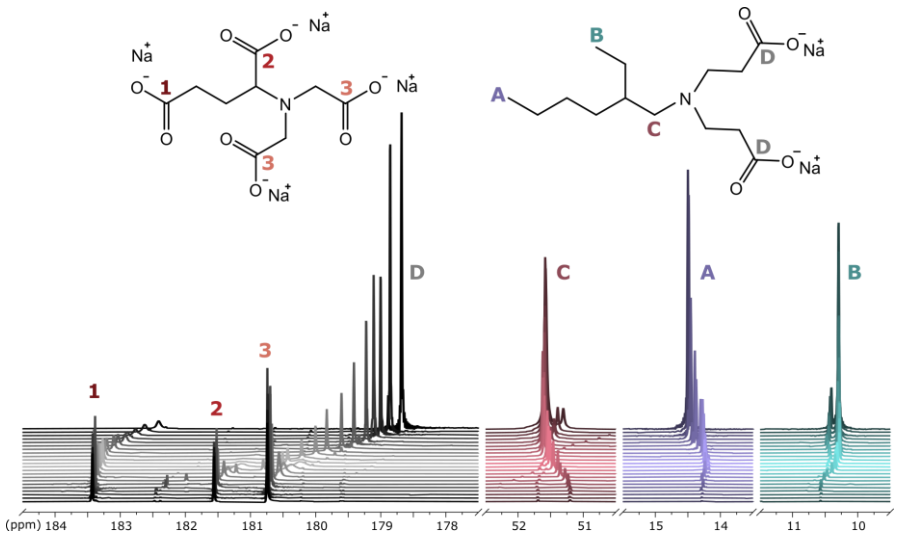

Figure 11. Molecular structures of BC8Amph and GLDA (top), and corresponding ^{13}C NMR spectra (below) for systems with 0.24 M GLDA and increasing BC8Amph concentration (from bottom to top).

The assigned peaks are indicated by numbers and letters in both the spectra and structures.

where stacked ^{13}C NMR spectra of the BC8Amph–GLDA system illustrate the progressive spectral changes observed upon increasing amphoteric surfactant concentration.

Across the stacked spectra, variations in both chemical shift and line width were observed for both species, with more pronounced changes occurring in the low-field region (left side of the spectra in Figure 11) corresponding to the carbons associated with the carboxylic groups in both the chelating agent and the amphoteric surfactant. The fact that the strongest perturbations occur in this region supports that these terminal, polar groups are directly involved in the interaction between the two molecules.

The changes in chemical shift of selected carbon atoms in the lipophilic chain of the surfactant molecule as the surfactant concentration varies reveal more details about the changes in microenvironment experienced by these atoms. Figure 12 presents the evolution of the chemical shift as a function of the

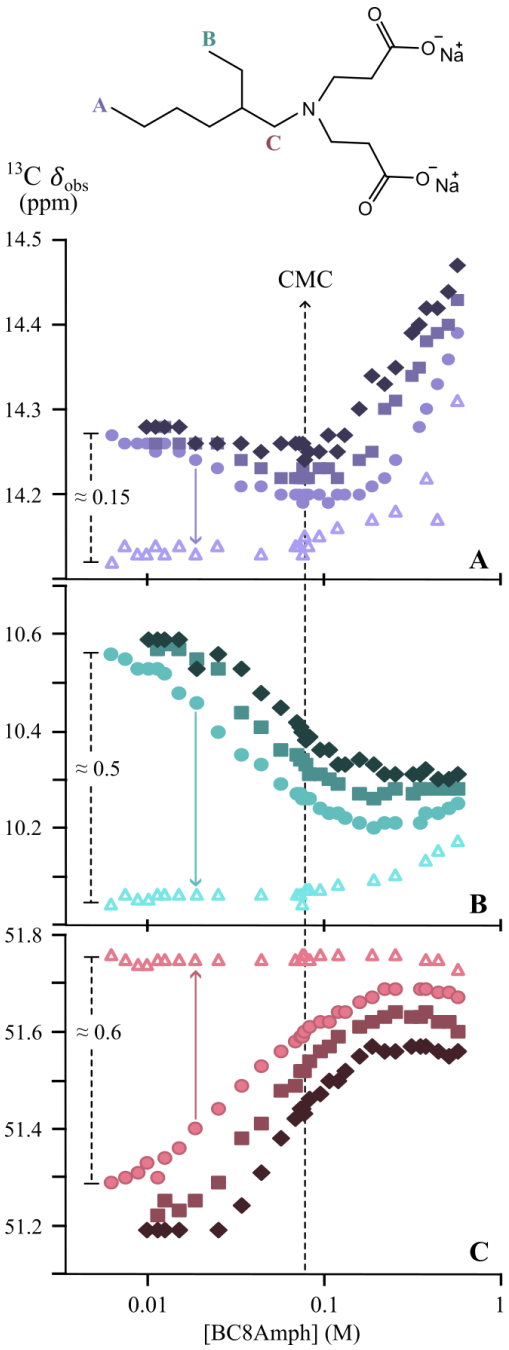

Figure 12. Chemical shift as a function of the surfactant concentration (BC8Amph) in systems without and with different GLDA concentrations (0.12 M, 0.24 M, and 0.36 M). The GLDA concentration is indicated in the graph by increasing the darkness of the symbols as the concentration increases. Each plot represents a distinct signal for carbon atoms in the lipophilic chain, color-coded as indicated in the molecule.

surfactant concentration, in systems either without GLDA or at different, but constant, GLDA concentrations.

The terminal carbon atoms of the surfactant (A and B in Figure 12) in the system without GLDA (non-filled symbols) illustrate the expected behavior for surfactant molecules undergoing micellization. At low surfactant concentration, their chemical shifts remain constant, consistent with the atoms residing in a uniform, polar environment where the surfactant exists predominantly as unimers. As the concentration increases, the curve displays an inflection, after which the chemical shifts move downfield. This transition follows the trend described by eq. (2) and reflects the progressive incorporation of these terminal groups into the apolar interior of surfactant associations. The observed shift marks the change in microenvironment during micellization, fully aligned with the expected behavior for surfactant solutions.[49]

The chemical shift changes of the carbon atom closest to the nitrogen group (C in Figure 12) further supports this interpretation. In the

system without GLDA, the shift shows little change as the concentration of surfactant increases, showing just a slight decrease once micelles form. This nearly constant trend reflects that the microenvironment of this carbon remains essentially unchanged, which remains at the micelle–water interface; no significant transition from a polar to an apolar environment occurs upon micellization.

The variation in chemical shift at increased GLDA concentration (filled symbols in Figure 12) displays a distinct pattern. A simple salting-in or salting-out additive would be expected to shift the chemical-shift curve and move the inflection point without altering the underlying trend. The change observed here, however, requires introducing additional terms into eq. (2), revealing an additional concentration-dependent process that is superimposed on the micellization behavior. Given that the system contains only water, GLDA, and amphoteric surfactant, this process must arise from interactions between GLDA and the surfactant, either in the unimer state or within surfactant associations. Considering these interacting species, eq. (2) can be revised as:

$$\delta_{\mathrm{obs}} = \delta_{\mathrm{u}}\left(\frac{C_{\mathrm{u}}}{C_{\mathrm{T}}}\right) + \delta_{\mathrm{m}}\left(\frac{C_{\mathrm{m}}}{C_{\mathrm{T}}}\right) + \delta_{\mathrm{u+ChA}}\left(\frac{C_{\mathrm{u+ChA}}}{C_{\mathrm{T}}}\right) + \delta_{\mathrm{m+ChA}}\left(\frac{C_{\mathrm{m+ChA}}}{C_{\mathrm{T}}}\right) \tag{7}$$

where the two new terms, $\mathrm{u} + \mathrm{ChA}$ and $\mathrm{m} + \mathrm{ChA}$, account for the surfactant interacting with the chelating agent (ChA) as a unimer (u) or in the micelle (m), respectively.

At low surfactant concentration, the magnitude of the chemical shift changes differs across the evaluated carbons, with atoms closer to the head group exhibiting more pronounced variations than those further along the lipophilic chain (Figure 12). This pattern aligns with the earlier observation that the strongest perturbations arise in the low-field region of the spectra, where the signal of polar groups of both GLDA and the surfactant are visible. Together, these changes indicate that GLDA interacts preferentially near the head group of the surfactant, where the chemical shift variations are more pronounced.

As the surfactant concentration increases while remaining below the CMC, the chemical shift responses exhibit a characteristic pattern (Figure 12). The terminal carbons shift upfield, with B showing the greatest change, whereas C near the head group shifts downfield. Importantly, all signals evolve progressively toward the chemical shifts of the GLDA-free system. In this concentration regime, eq. (7) simplifies to the unimer contributions alone, since micelles are not present. The convergence toward the GLDA-free chemical shifts therefore indicates that the relative fraction of non-interacting surfactant unimers increases. This behavior is consistent with a dynamic equilibrium in which added surfactant progressively remains unbound to GLDA, which can be described by:

below CMC:

$$[S_u] + [ChA] \rightleftharpoons [S_u \cdot ChA] \tag{8}$$

and above CMC:

$$[S_u] + [S_m] + [ChA] \rightleftharpoons [S_u \cdot ChA] + [S_m \cdot ChA] \tag{9}$$

where $S_u \cdot ChA$ and $S_m \cdot ChA$ refers to the complex formed between the chelating agent and the unimer, and a surfactant belonging to a micelle, respectively.

At higher surfactant concentrations, the system enters a final regime in which the chemical-shift trends diverge. The terminal carbon (A), located at the far end of the lipophilic chain, continues to shift downfield as the proportion of molecules residing in the apolar micellar core increases, which is aligned with a progressive transition to a hydrophobic environment. Conversely, B and C that are closer to the micelle surface, experience a more complex microenvironment. Here, their surroundings consist of the lipophilic core of the micelle, water molecules near the head group, and neighboring GLDA molecules. The resulting leveling off behavior of the chemical shift reflects contributions from all these surrounding factors.

4.3. Effect of Headgroup and Chelating Agent Structure

This section expands the preceding discussion by analyzing the low-field region of the ^{13}C NMR spectra, corresponding to the polar functional groups of both species and exhibiting the most substantial spectral perturbations. These changes provide a basis for understanding how molecular structure dictates the nature and strength of the interactions between the amphoteric surfactant and the chelating agent. A broader set of compounds is included, with their structures and abbreviations shown in Figure 13

To clarify the contribution of nitrogen to the interaction, systems containing sodium citrate, a structurally similar

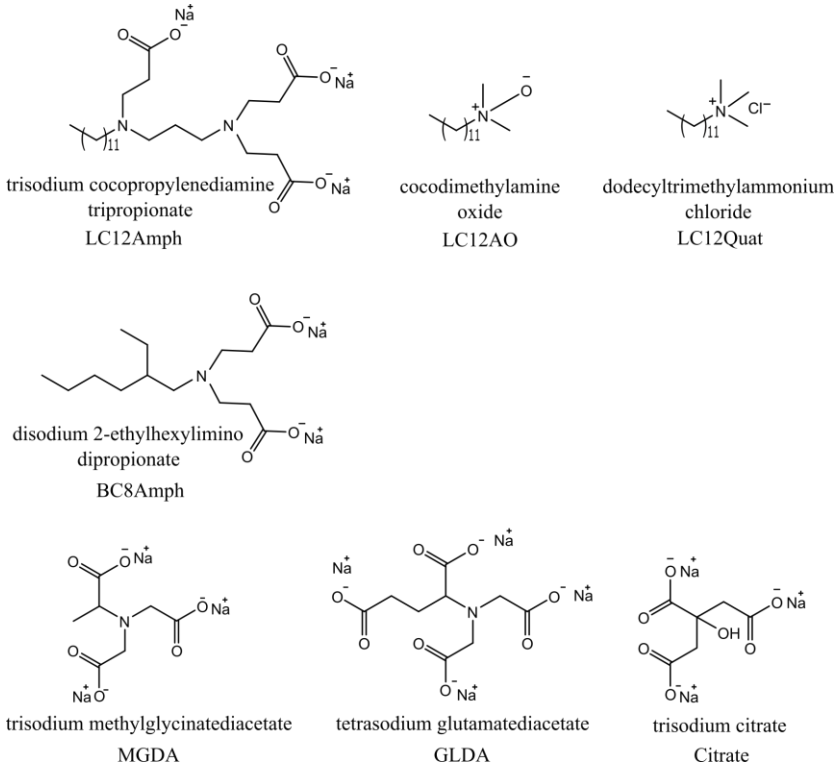

The selection criteria prioritized commercially relevant compounds with minimal structural variation to isolate the effects of specific molecular features.

Figure 13. Chemical structures of the chelating agents and surfactants evaluated. The abbreviated names used are included for clarity.

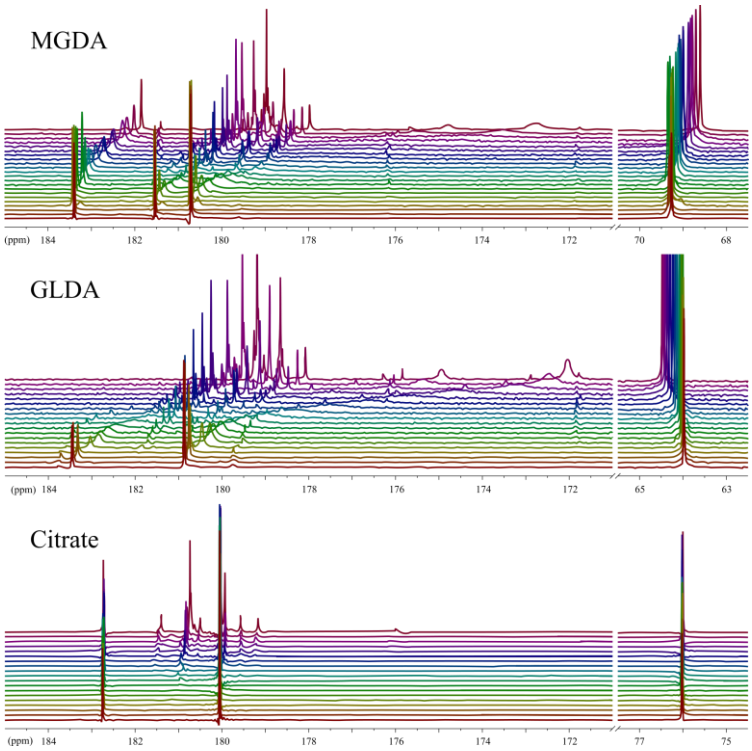

Figure 14. Comparison of relevant ^{13}C NMR regions for systems containing 0.24 M of chelating agent (from top to bottom: MGDA, GLDA, and citrate), and varying concentrations of LC12Amph. The surfactant concentration increases from bottom to top in each stacked ^{13}C NMR spectrum.

polycarboxylate that lacks nitrogen, were evaluated alongside MGDA and GLDA in the presence of LC12Amph (Figure 14).

In citrate-containing systems, the ^{13}C signals remain effectively unchanged, showing neither notable shifts nor broadening. This contrast indicates that the nitrogen atom is essential for enabling the interaction observed in systems containing MGDA or GLDA.

The influence of the negatively charged moiety, and specifically its distance from the nitrogen, was assessed using two complementary approaches: first, by analyzing the chemical shift changes among the carboxylic carbons in GLDA (Figure 15), and second,

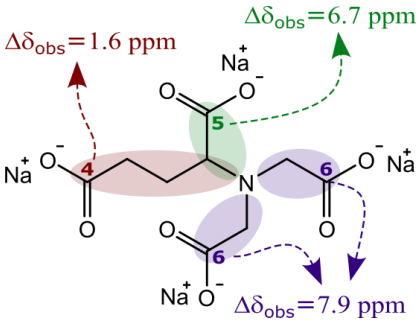

Figure 15. Chemical shift changes for each carboxylic carbon in GLDA, mapped onto the molecular structure to illustrate both their relative separation from the nitrogen atom and the influence of adjacent substituents.

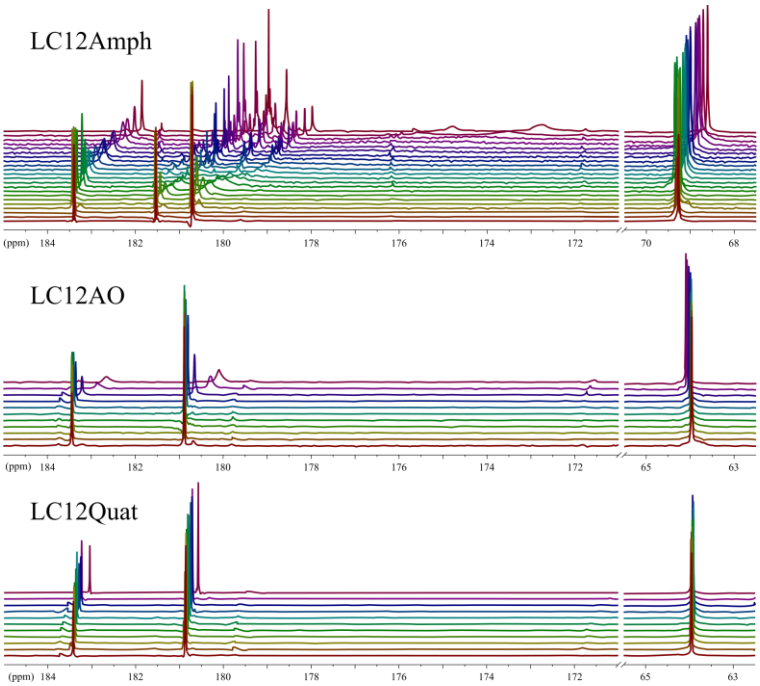

Figure 16. Comparison of relevant ^{13}C NMR regions for systems containing 0.24 M MGDA and varying concentrations of LC12Amph, LC12AO, and LC12Quat (displayed top to bottom). The surfactant concentration increases from bottom to top in each stacked ^{13}C NMR spectrum.

by comparing the behavior of MGDA with different surfactants, namely LC12Amph, LC12AO, and LC12Quat (Figure 16).

In the GLDA case, the position of the carboxylic groups relative to the nitrogen is central. Carbons C5 and C6 are separated from the nitrogen by one carbon atom, whereas C4 is separated by three. C4 shows markedly smaller chemical shift changes, 1.6 ppm compared with 6.7 and 7.9 ppm for C5 and C6 respectively (Figure 15). C4 also exhibits reduced signal broadening. These observations indicate that the interaction becomes less favorable when the nitrogen and the carboxylate groups are separated by a greater distance.

In the second approach (Figure 16), MGDA displays substantial chemical shift changes and pronounced

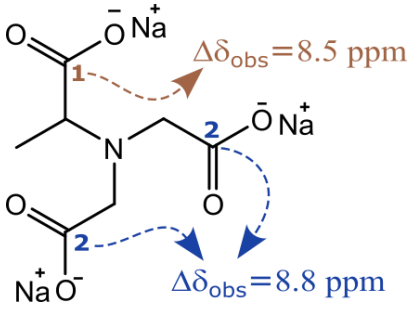

Figure 17. Chemical shift changes observed for each carboxylic carbon in MGDA, mapped onto the molecular structure to illustrate the influence of substituents near the carboxyl groups.

broadening in the presence of LC12Amph, but only minor shifts with LC12AO and LC12Quat. This difference suggests that efficient interaction requires a surfactant head group carrying both positive and negative charges. Furthermore, the spatial arrangement of these charges must fall within a suitable range, neither too short as found in amine oxides nor too extended as in the longest chain of GLDA. Differences in electronic density between head group types may further modulate the interaction, with amine oxides being electronically harder and less delocalized than the softer carboxylates.[80]

Steric constraints can influence both the likelihood and extent of interaction between a chelating agent and a surfactant. To assess these effects, pairs of chemically comparable carbonyl groups in GLDA and MGDA are considered (Figures 15 and 17). In the absence of steric interference, such carbonyls would be expected to exhibit similar chemical shift changes when exposed to the same surfactant. For GLDA, this applies to the C5–C6 pair, and for MGDA to the C1–C2 pair. By comparing the behavior of carbons adjacent to substituents (C1 in MGDA and C5 in GLDA) with their unsubstituted counterparts (C2 and C6), the impact of local steric environments can be evaluated.

In GLDA, C5 exhibits substantially smaller changes than C6, approximately 1.2 ppm, corresponding to roughly 20 percent of the total variation, whereas MGDA displays a more modest difference between C1 and C2. These trends reflect differences in the substituents adjacent to the carbonyl groups: C5 is neighbored by a bulkier propionic acid unit, whereas C1 is adjacent only to a methyl group. The larger substituent imposes greater steric congestion, reducing the accessibility of the carbonyl site and thereby limiting the extent of interaction. In the case of a methyl substituent, steric effects are weak and may be outweighed by a slight electronic stabilization due to its electron-donating character, thereby helping to explain why the net chemical shift difference between C1 and C2 remains small.

In parallel, comparison of line broadening for each pair (C5 vs. C6 and C1 vs. C2) yields similar broadening profiles (Paper II), indicating that once the interaction occurs, the effective interaction strength is comparable across the sterically distinct sites. This supports the interpretation that steric hindrance primarily governs the probability of interaction by restricting spatial accessibility, whereas the inherent strength of the interaction, once formed, remains largely unaffected.

4.4. Influence of the Lipophilic Chain: Role of Surfactant Hydrophobic Structure

By comparing the behavior of MGDA and GLDA in the presence of BC8Amph and LC12Amph within equivalent binary systems, the influence of surfactant tail architecture on the interaction can be evaluated. Although these systems display similar changes in chemical shift (Paper II), the width of the signal provides further details. Pronounced differences in the line-broadening trends, used here as a qualitative measure of interaction strength, reveal that the nature of the

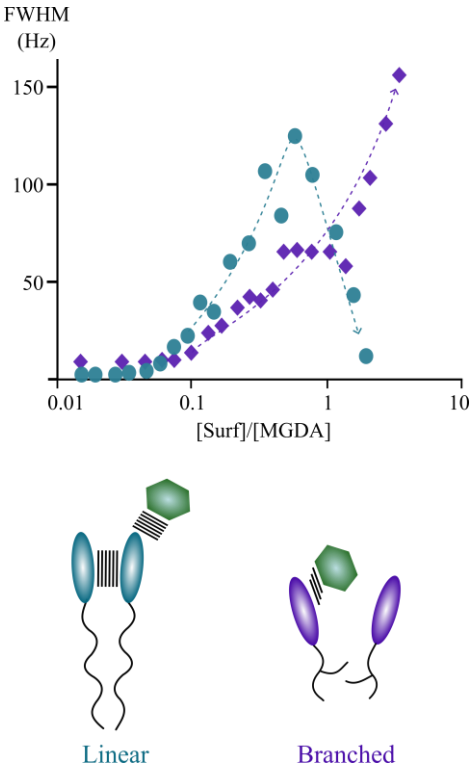

Figure 18. Top: Signal width at half-maximum as a function of surfactant-to-chelating agent ratio for LC12Amph and BC8Amph. Bottom: Schematic illustrating how surfactant tail structure and packing influence interaction strength.

hydrophobic chain significantly modulates the interaction.

Figure 18 illustrates these effects by presenting the evolution of signal width as a function of the surfactant-to-chelating agent ratio, together with a schematic representation of the proposed interaction motifs. For LC12Amph, line broadening increases with concentration until reaching a well-defined maximum, after which it decreases. BC8Amph, in contrast, produces a steady and monotonic increase in broadening across the full concentration range.

These differences reflect the structural characteristics of the two amphoteric surfactants. LC12Amph, with its long linear tail, forms compact and relatively well-packed micelles whose curvature is already constrained by the hydrophobic chain geometry. Under these conditions, the addition of GLDA does not produce a significant curvature adjustment that would compensate for the energetic cost of incorporating the chelating agent at the interface. As a result, the system experiences a penalty when GLDA remains organized along the micellar surface rather than freely diffusing in solution, and the apparent interaction remains limited.

The branched tail of BC8Amph restricts efficient packing and leads to aggregates that are more deformable than those formed by LC12Amph. Upon addition of GLDA, these aggregates can reduce solvophobic stress by reorganizing into structures with a more favorable curvature, effectively burying the hydrophobic tails more deeply. This curvature adjustment lowers the interfacial free energy, making association with the chelating agent energetically advantageous. The resulting CPP-driven reorganization manifests as a stronger apparent interaction with GLDA across the entire concentration range.

The difference between the two amphoteric surfactants becomes more pronounced in ternary systems containing a linear, poorly water-soluble nonionic surfactant. Diffusion NMR data (Figure 19) show that LC12Amph and BC8Amph adopt markedly different roles.

The linear amphoteric displays a signal attenuation slope in the Stejskal–Tanner plot that closely matches that of the nonionic surfactant, demonstrating that both species diffuse together as part of mixed micelles. The branched amphoteric exhibits a substantially more negative slope, which can be interpreted as a much lower apparent fraction incorporated into the micellar phase, if incorporated at all. These results indicate two distinct solubilization mechanisms: the linear amphoteric acts as a genuine surfactant, associating with the nonionic surfactant to form mixed micelles, whereas the branched amphoteric behaves as a hydrotrope under the studied conditions, enhancing solubility without substantial incorporation into micelles.

In ternary systems, the diffusion behavior of GLDA further highlights the diverging roles of the two amphoteric surfactants. In systems containing the linear amphoteric surfactant, GLDA displays two clearly resolved slopes in the Stejskal–Tanner analysis. One slope matches that of the nonionic and amphoteric surfactants, reflecting the micelle-associated

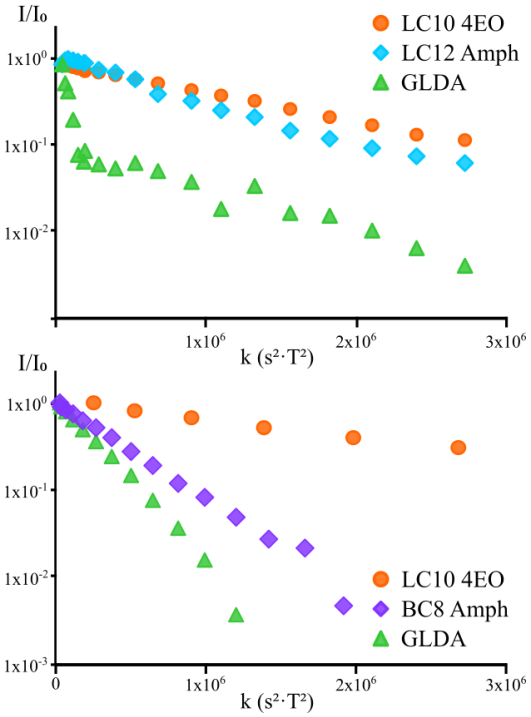

Figure 19. Stejskal–Tanner plots for ternary systems containing nonionic surfactant, amphoteric surfactant, and GLDA. Top: linear amphoteric (40 mM); bottom: branched amphoteric (190 mM). Symbols correspond to different species: nonionic surfactant (circles), amphoteric surfactant (diamonds), and GLDA (triangles).

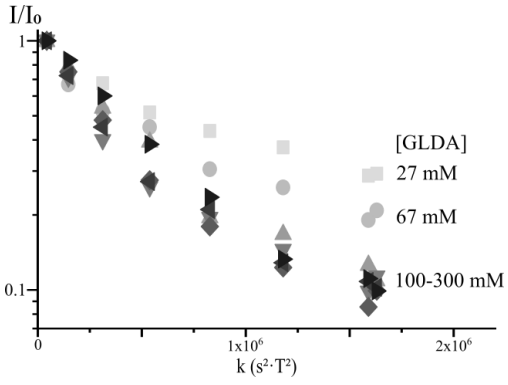

Figure 20. Stejskal–Tanner plots (I/I_0 versus scaled k value) showing how the apparent self-diffusion of GLDA changes with concentration in ternary systems composed of LC12Amph and LC10 4EO. Darker symbols indicate higher GLDA concentrations.

population; the second corresponds to the faster diffusion of GLDA free in solution. The presence of two distinct components indicates slow exchange between free and micelle-bound GLDA, consistent with a relatively strong or long-lived interaction.

In systems containing the branched amphoteric surfactant, GLDA exhibits a single monoexponential attenuation, which indicates either fast exchange between bound and free states or a negligible bound fraction. Both interpretations point to a weaker and more transient interaction between GLDA and BC8Amph.

As the concentration of GLDA is increased, its interaction with the micellar system evolves in a systematic and reproducible manner (Figure 20). At low GLDA concentrations, the observed diffusion reflects a substantial contribution from micelle-associated GLDA under fast exchange conditions. Because micelle-associated species diffuse more slowly than freely dissolved GLDA, the resulting population-averaged diffusion coefficient is reduced, yielding relatively shallow slopes in the Stejskal–Tanner plots. As the GLDA concentration is increased, additional chelating agent is no longer accommodated within micelle-associated environments but remains predominantly in bulk. This progressively increases the contribution of the fast-diffusing population to the NMR signal, leading to steeper slopes and an apparent increase in the diffusion coefficient. Beyond a characteristic concentration threshold, the diffusion behavior becomes invariant, indicating that the relative population of micelle-associated GLDA has reached a constant value and that further additions of GLDA do not alter the exchange-weighted diffusion response.

The emergence of a concentration-independent diffusion regime at higher GLDA concentrations indicates that the micellar system offers a finite number of favorable interaction environments for GLDA, which become progressively occupied as the chelating agent concentration increases. Once these environments are saturated, the overall micellar organization and the exchange dynamics between associated and non-associated GLDA

remain largely unchanged, even as the total GLDA concentration continues to rise. The concentration-dependent evolution of GLDA diffusion therefore reflects a redistribution process in which micelle-associated GLDA contributes measurably to the diffusion signal only up to the point at which available interaction sites are occupied; beyond this point, the bulk population dominates the observed response.

As the association of GLDA with the micellar system reaches a limiting regime, attention naturally shifts to how the micellar aggregates themselves respond to the presence of the chelating agent. This response can be probed by following the diffusion of the nonionic surfactant. Extending the discussion beyond linear systems, the inclusion of a branched nonionic analogue allows the role of hydrophobic chain branching in both surfactant components to be evaluated in shaping the micellar response to GLDA.

The evolution of nonionic surfactant diffusion with increasing GLDA concentration (Figure 21) reveals a clear ordering of responses. Mixed micelles composed of linear amphoteric and linear nonionic surfactants display a pronounced decrease in diffusion as GLDA is added, indicating substantial micellar restructuring. When branching is introduced in either the amphoteric or the nonionic surfactant, this response becomes progressively weaker, and in systems where both components are branched, the diffusion of the nonionic surfactant remains essentially unchanged across the investigated GLDA concentration range.

In systems containing the linear amphoteric surfactant, the initial additions of GLDA induce only minor changes in micellar diffusion, while a marked reduction is observed once the chelating agent concentration exceeds a characteristic threshold. This delayed response mirrors the concentration regime in which GLDA association with the micelles becomes significant, suggesting a coupling between chelating agent partitioning and aggregate restructuring. In comparison, when the branched amphoteric surfactant is combined with

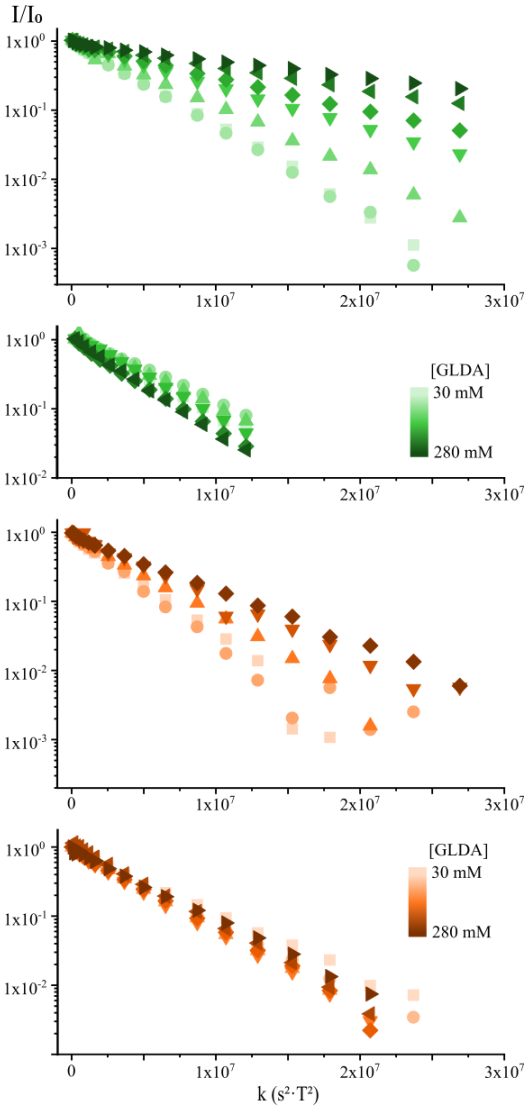

Figure 21. Stejskal–Tanner plots illustrating changes in the apparent self-diffusion behavior of the nonionic surfactant upon GLDA addition in ternary systems. Panels are arranged from top to bottom as LC12Amph–LC10 4EO, LC12Amph–BC10 5EO, BC8Amph–LC10 4EO, and BC8Amph–BC10 5EO. Darker symbols correspond to higher GLDA concentrations.

the linear nonionic surfactant, a modest but reproducible increase in diffusion is observed upon GLDA addition, pointing to a distinct mode of micellar adjustment.

The ability of the micellar system to reorganize in response to the presence of GLDA is governed by the degree of hydrophobic chain branching. Micelles formed with linear amphoteric surfactants display greater structural adaptability, consistent with more efficient packing and enhanced capacity for growth or elongation. Introducing hydrophobic chain branching reduces this flexibility, thereby suppressing GLDA-induced changes in diffusion.

Since the micellar diffusion in BC8Amph-LC10 4EO system deviates from the rest, the changes in micellar diffusion cannot be attributed solely to the response of the nonionic component. To resolve this apparent discrepancy, the diffusion of the branched amphoteric surfactant itself is examined as GLDA increases (Figure 22), both in the presence of linear and branched nonionic surfactants.

In both cases, the diffusion coefficient of BC8Amph decreases steadily with increasing GLDA concentration, indicating a systematic reduction in its mobility. This trend is more pronounced when the branched nonionic surfactant is present, but it is clearly visible for both nonionic architectures. The monotonic decrease differs from the relatively weak, or in some cases opposite, trends observed for the nonionic surfactant. This behavior points to a redistribution of the amphoteric component within the system.

The nearly unchanged diffusion of GLDA (Paper IV), and the modest increase of nonionic diffusion observed in systems containing BC8Amph, suggest that increasing GLDA concentration promotes incorporation of BC8Amph into the micellar population under fast exchange conditions. As the amphoteric surfactant becomes increasingly associated with micelles, its apparent diffusion decreases, while the micellar aggregates themselves become smaller or more dynamic. This redistribution reconciles the different diffusion trends of the individual components and highlights that, in

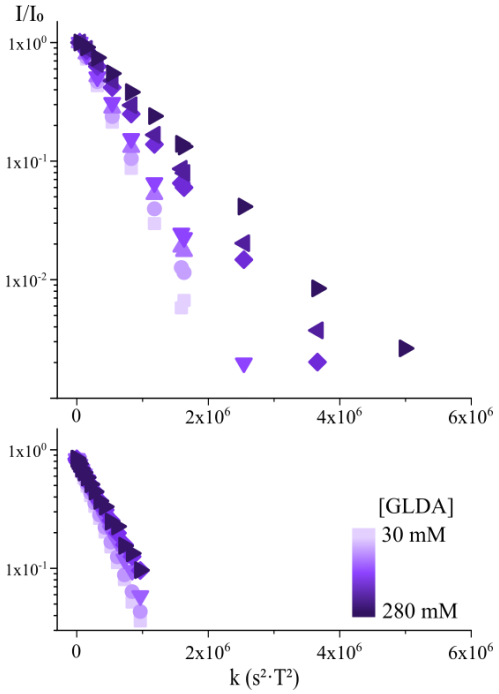

Figure 22. Stejskal–Tanner plots (I/I_0 versus scaled k value) showing the apparent self-diffusion behavior of BC8Amph as a function of GLDA concentration in ternary mixed surfactant systems. The top panel corresponds to systems containing the branched nonionic surfactant BC10 5EO, while the bottom panel corresponds to systems containing the linear nonionic surfactant LC10 4EO. Increasing symbol darkness indicates increasing GLDA concentration.

branched amphoteric systems, micellar restructuring proceeds primarily through changes in surfactant partitioning.

Taken together, these observations show that branching in the surfactant tail plays a central role in determining the mode and extent of interaction with chelating agents. In binary systems, the branched amphoteric promotes stronger apparent interactions because its less compact, more deformable micelles experience greater packing frustration. The addition of chelating agent enables these assemblies to reorganize toward a curvature that better shields the hydrophobic region, thereby reducing solvophobic stress. This curvature adjustment drives the stronger interaction observed for BC8Amph.

In ternary systems, however, the situation is completely different. The linear amphoteric, combined with the linear nonionic surfactant, forms larger mixed micelles whose curvature and packing can be efficiently modulated upon GLDA addition. In this case, the system can lower its interfacial free energy by adjusting the critical packing parameter, reorganizing into smaller and more spherical micelles as GLDA becomes increasingly incorporated. In consequence, the linear amphoteric displays stronger interaction in the ternary mixtures, reflecting a curvature-driven redistribution of packing.

4.5. Mesoscopic Manifestations of Surfactant–Chelating Agent Interactions

While molecular-scale interactions determine the affinity between surfactants and chelating agents, the consequences of these interactions ultimately manifest at the mesoscopic level through changes in micellar size, shape, and internal organization. SANS was therefore employed to examine how variations in hydrophobic chain architecture and GLDA concentration influence the structure of mixed micelles in the ternary systems investigated in this work.

Across all formulations, the SANS profiles (Figure 23) are characteristic of well-defined micellar aggregates. The high-q region is dominated by a q^{-4} decay, indicating sharp micellar interfaces, while the low-q region generally exhibits a plateau consistent with isolated or weakly interacting aggregates. In some systems, subtle deviations from this idealized behavior are observed, including weak oscillations associated with finite aggregate size and, in selected cases, low-q upturns or faint correlation peaks. These features point to modest intermicellar interactions arising from electrostatic repulsions or weak attractive forces, but they do not dominate the scattering response.

Rather than focusing on general scattering features, the SANS analysis was directed toward extracting physically meaningful parameters describing aggregate size and shape (Figure 24). The apparent micellar volume was estimated from the forward scattering intensity, enabling calculation of an apparent molar mass and corresponding aggregation number. Although these values depend on model assumptions, they

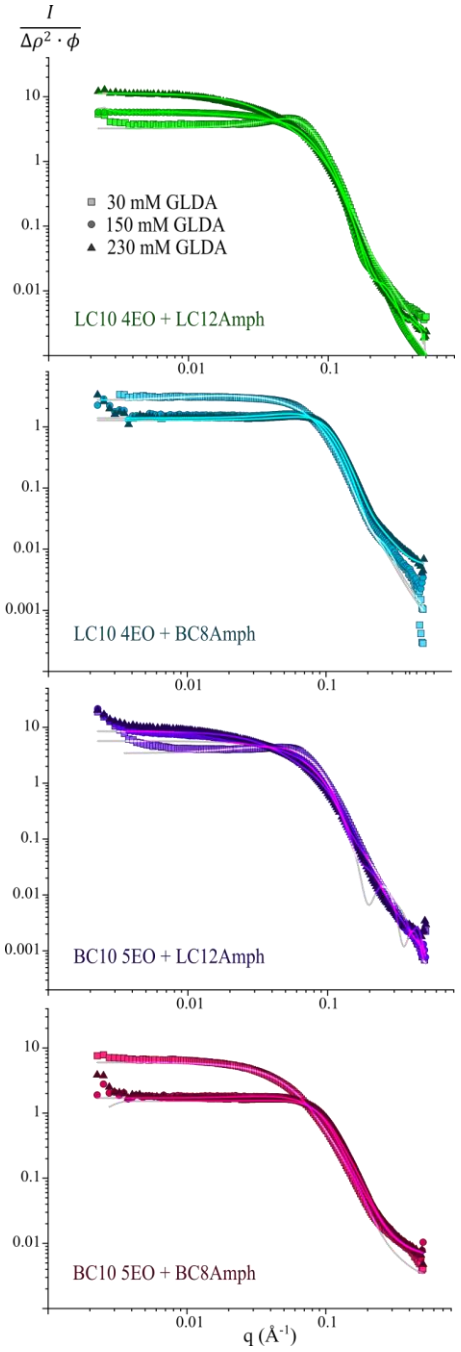

Figure 23. Normalized SANS profiles ($I/\phi\Delta\rho^2$ as a function of q) for ternary surfactant systems containing linear or branched nonionic surfactants mixed with linear or branched amphoteric surfactants at increasing GLDA concentration. Experimental data are shown as symbols, with darker symbols corresponding to higher GLDA concentrations, while solid lines indicate fits obtained using the selected micellar form-factor models.

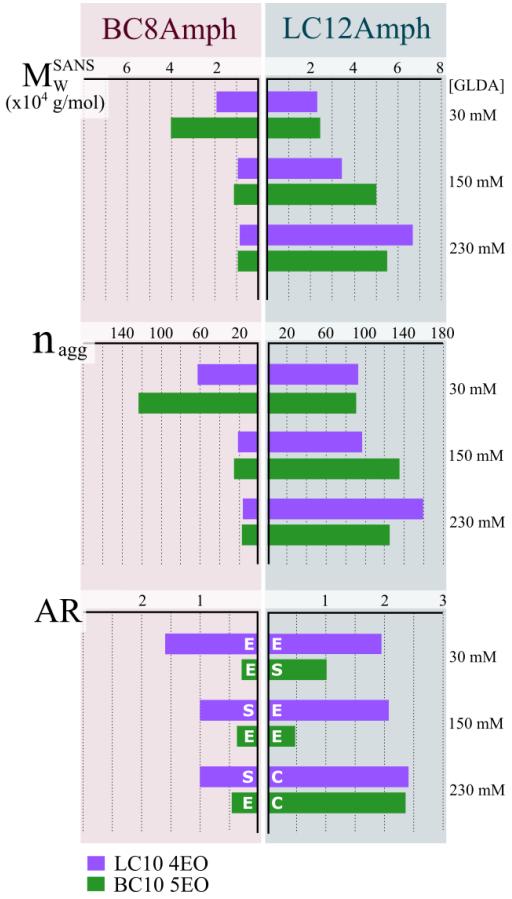

Figure 24. Micellar molar mass M_w determined by SANS (top panels), aggregation number calculated from I_0 (middle panels), and micellar aspect ratio (bottom panels) as a function of GLDA concentration for mixed surfactant systems. Left panels correspond to systems containing the branched amphoteric surfactant BC8Amph, while right panels correspond to systems containing the linear amphoteric surfactant LC12Amph. Purple and green bars denote systems containing LC10 4EO and BC10 5EO, respectively. Letters S, E, and C indicate the form-factor model used for fitting (sphere, ellipsoid, and cylinder).

provide a robust comparative framework for assessing relative changes across systems of different composition.

A clear and systematic influence of hydrophobic chain architecture emerges from this analysis. Independent of GLDA concentration, systems containing branched surfactants form smaller aggregates with lower aggregation numbers than their linear counterparts. This behavior is consistent with the reduced packing efficiency imposed by hydrophobic branching, which limits the number of chains that can be accommodated within the micellar core and constrains the extent to which curvature can relax.

This effect on the architecture of the aggregates is particularly evident when comparing systems containing the branched amphoteric surfactant BC8Amph with those containing the linear amphoteric surfactant LC12Amph. In the presence of BC8Amph, micellar molar masses and aggregation numbers remain comparatively low and decrease further as the GLDA concentration increases. This trend supports the conclusion, drawn earlier from diffusion NMR

measurements, that BC8Amph interacts only weakly with the micelles and remains largely in the bulk phase. Increasing GLDA concentration does not promote micellar growth in these systems but instead modifies the solvent environment, enhancing the solubility of the nonionic surfactant and leading to a net reduction in aggregate size.

Systems containing LC12Amph display a markedly different response. Here, both the apparent molar mass and aggregation number increase with increasing GLDA concentration, particularly at high GLDA levels. These changes are accompanied by pronounced alterations in micellar shape. Whereas micelles are close to spherical at low GLDA concentration, they progressively evolve into ellipsoidal or short cylindrical aggregates as the chelating agent content increases, with characteristic dimensions extending up to approximately 100–120 Å. This restructuring reflects the effective incorporation of LC12Amph into mixed micelles and highlights the ability of linear hydrophobic chains to accommodate reduced curvature through elongation of the micellar core.

The contrast between these two behaviors underscores the dual role of GLDA in the system. At low to intermediate concentrations, GLDA primarily engages in specific interactions with amphoteric headgroups, driving micellar restructuring without substantial growth. At higher concentrations, more generic salting-out effects dominate, promoting micellar enlargement and, in systems capable of accommodating it, transitions toward lower-curvature morphologies.

Branched–branched systems represent a limiting case in which curvature relaxation is strongly suppressed. When described using ellipsoidal form factors, these systems consistently yield aspect ratios below unity across the full GLDA concentration range, indicating aggregates that remain close to isotropic and do not develop pronounced elongation. Such behavior is indicative of strong packing frustration within the micellar

core, imposed by hydrophobic branching, which inhibits directional growth even under conditions that promote elongation in linear systems.[81–84]

At intermediate and high GLDA concentrations, these branched–branched systems converge toward similar molar masses and aggregation numbers that remain lower than those observed at low GLDA concentration. This behavior aligns with diffusion NMR observations showing that, with increasing GLDA concentration, BC8Amph exhibits reduced self-diffusion while the nonionic surfactants diffuse more rapidly. These opposing trends indicate that GLDA promotes closer association of the amphoteric surfactant with the micellar population, leading to enhanced modification of the local solvent environment surrounding the micelles. The resulting changes in solvation favor improved solubility of the nonionic surfactant and are accompanied by a slight reduction in micellar size rather than aggregate growth.

4.6. Effect of the Interactions on Bulk and Surface Properties

The mesoscopic restructuring of surfactant aggregates described above provides a direct framework for understanding how molecular interactions translate into macroscopic formulation properties in the presence of chelating agents. Accordingly, this section examines both ternary systems comprising a nonionic surfactant, an amphoteric surfactant, and a chelating agent, as well as binary amphoteric–chelating agent systems. Particular emphasis is placed on cloud point and viscosity, which are highly sensitive to micellar size, shape, and hydration, studied by SANS and DLS.

Figure 25 illustrates the evolution of cloud point and viscosity upon addition of GLDA or MGDA to representative surfactant systems. When a water-soluble nonionic ethoxylated surfactant is used, increasing chelating agent concentration leads to a progressive decrease in cloud point, accompanied by an increase in viscosity. This behavior is attributed to a

salting-out mechanism, whereby the chelating agent competes for water molecules that would otherwise hydrate the ethoxylated head groups. The resulting reduction in hydration lowers the solubility of the nonionic surfactant and promotes micellar growth, which in turn increases solution viscosity.

For poorly soluble nonionic surfactants such as LC10 4EO, the presence of a solubilizing agent is required to obtain clear solutions. When an anionic surfactant, such as sodium dodecyl sulphate, is used as a solubilizer, a high cloud point is observed at low chelating agent concentration. However, increasing GLDA concentration causes a sharp decrease in cloud point together with a steep rise in viscosity. This response aligns with the well-established behavior of ionic surfactants in the presence of electrolytes, where electrostatic screening reduces head-group repulsion, facilitates micellar growth, decreases solubility, and increases viscosity. The same pattern is observed for systems containing LC12Quat or LC12AO as solubilizers, as well as in LC12Amph-Citrate combinations (Paper II).

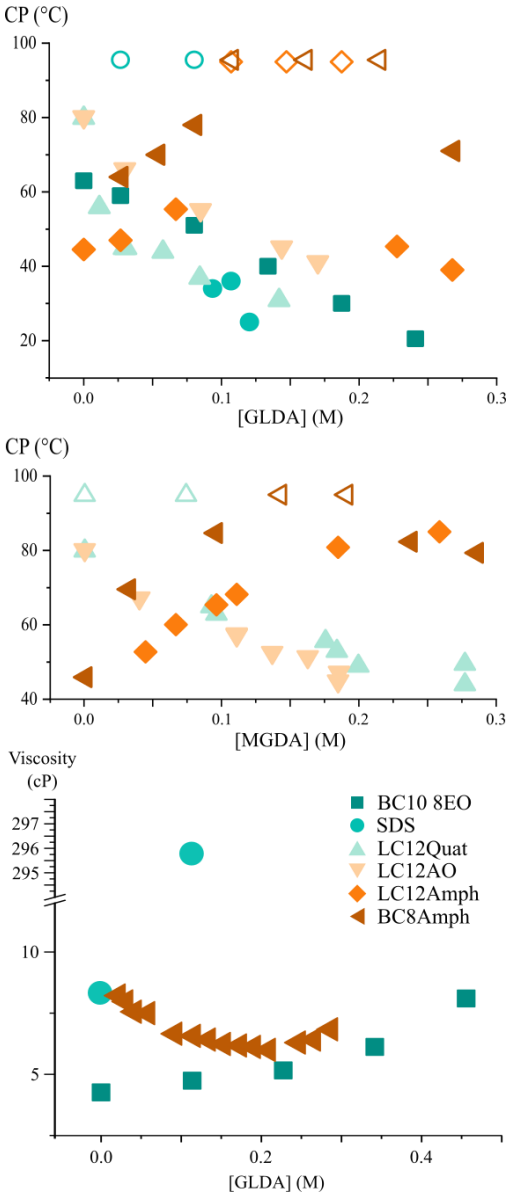

Figure 25. Evolution of cloud point and viscosity with increasing chelating agent concentration in mixed surfactant systems. Cloud point as a function of GLDA concentration (top) and MGDA concentration (middle), and viscosity as a function of GLDA concentration (bottom), for formulations containing either a soluble nonionic surfactant (BC10 8EO) or a poorly soluble nonionic surfactant (LC10 4EO) solubilized by anionic, cationic, amine oxide, or amphoteric surfactants. Open symbols indicate cloud point values above 85 °C.

A markedly different macroscopic response is observed when amphoteric surfactants are used as solubilizers in systems containing either GLDA or MGDA (Figure 25). In these systems, the cloud point initially increases with chelating agent concentration, reaching a maximum, before decreasing at higher concentrations. Over the same concentration range, viscosity passes through a minimum. This combination of increased solubility and reduced viscosity stands in clear opposition to the classical salting-out behavior observed for ionic systems.

Considering that viscosity generally increases with micellar size, while cloud point decreases, and taking into account the diffusion NMR evidence presented earlier, these macroscopic trends are consistent with a reduction in micellar size upon addition of chelating agents to amphoteric-stabilized systems. Such a reduction can be rationalized by an effective increase in the area occupied by the surfactant head group due to complex formation between the chelating agent and the amphoteric head group. This increase in head-group area lowers the critical packing parameter, favoring the formation of smaller, more spherical micelles and thereby explaining the observed increase in cloud point and decrease in viscosity.

When combined with insights extracted from micro- and mesoscopic evaluations, these observations allow the identification of three distinct interaction regimes governing the response of amphoteric–chelating agent surfactant systems. These regimes are hereafter referred to as the interaction-limited, interaction-saturated, and salting-out regimes. In terms of cloud point behavior, the interaction-limited regime is characterized by a pronounced increase in cloud point with increasing chelating agent concentration, the interaction-saturated regime by a plateau in cloud point, and the salting-out regime by a subsequent decrease in cloud point as electrolyte effects dominate.

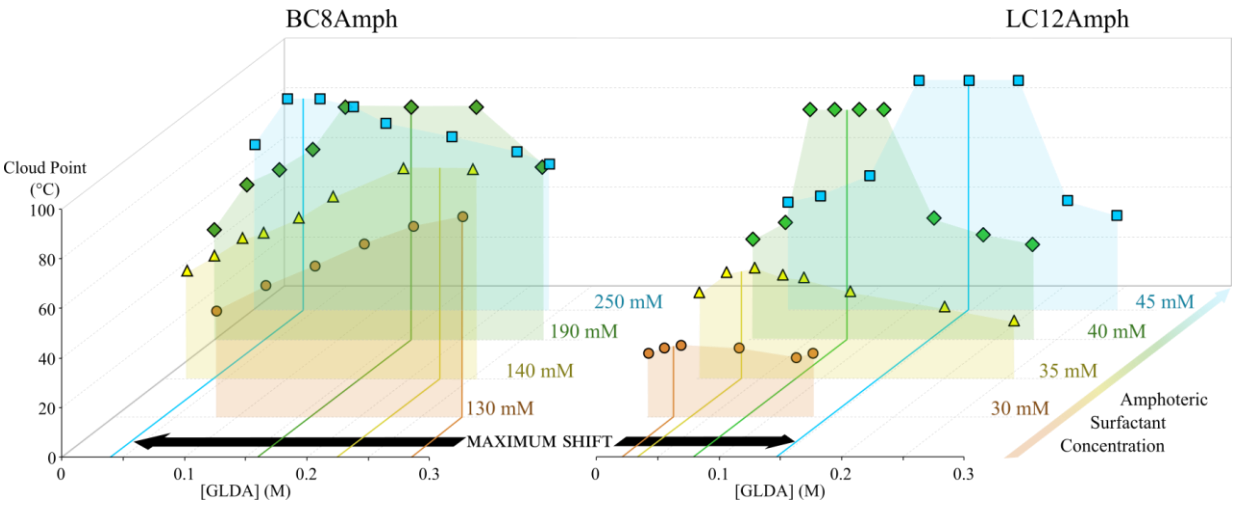

Figure 26. Cloud point behavior of nonionic ethoxylated surfactants in mixed systems with amphoteric surfactants upon addition of GLDA. The left panel shows systems containing BC8Amph (left), and LC12Amph (right), illustrating how amphoteric tail architecture and

A comparison of the evolution of the cloud point behavior in ternary systems containing either branched (BC8Amph) or linear (LC12Amph) amphoteric surfactants provides further insight into how these molecular interactions translate into macroscopic formulation properties. Figure 26 summarizes the cloud point response as a function of chelating agent concentration at different amphoteric surfactant concentrations, revealing distinct trends that depend strongly on amphoteric chain architecture.

For systems containing BC8Amph, increasing amphoteric surfactant concentration shifts the interaction-saturated regime, identified by the cloud point maximum, toward lower GLDA concentrations. This trend reflects a decreasing nonionic-to-amphoteric ratio, which progressively reduces the influence of interaction-driven changes in hydrophilicity on overall solubility. At sufficiently high BC8Amph concentrations, these interaction effects become minor and conventional salting-out behavior dominates the cloud point response.

Systems containing LC12Amph exhibit a more complex evolution. At low amphoteric concentrations, the cloud point remains nearly constant at low GLDA levels and decreases at higher chelating agent concentrations, indicating that salting-out effects prevail when incorporation of the amphoteric surfactant into micelles is limited. As the LC12Amph

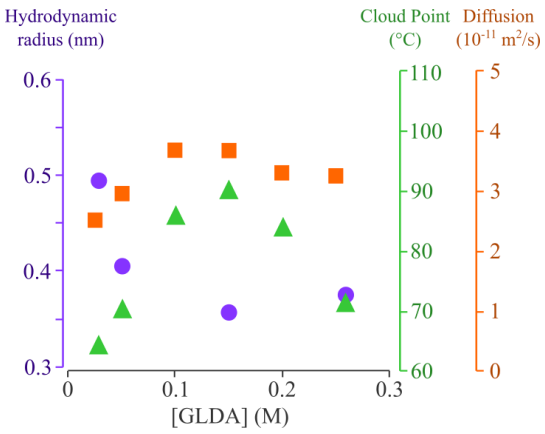

Figure 27. Hydrodynamic radius (circles), diffusion coefficients (squares), and cloud point temperatures (triangles) as a function of GLDA concentration for ternary systems containing constant concentrations of nonionic and amphoteric surfactants.

concentration increases, however, the cloud point behavior increasingly resembles that observed for BC8Amph systems; however, the interaction-saturated regime shifts toward higher GLDA concentrations. This shift reflects the formation of mixed micelles in which LC12Amph is efficiently incorporated. In such assemblies, GLDA associates with amphoteric headgroups at the micelle surface, increasing the effective hydrophilic area and promoting curvature adjustments that relieve packing constraints in larger aggregates. As the population of amphoteric headgroups grows, higher chelating agent concentrations are required to induce comparable restructuring of the micelle.

DLS measurements provide complementary support for this interpretation by capturing changes in the hydrodynamic size of the aggregates as formulation composition is varied. The observed trends in hydrodynamic radius (Figure 27) closely mirror those inferred from SANS, diffusion NMR, cloud point, and viscosity measurements. Systems in which micelles remain small or decrease in size with increasing GLDA exhibit higher

cloud points, lower viscosity, and faster nonionic surfactant diffusion, whereas conditions associated with micellar growth are reflected in larger hydrodynamic radii. In this sense, DLS serves as an independent validation that the solubilization mechanisms and aggregate restructuring identified at the mesoscopic level are directly linked to bulk formulation behavior.

Beyond bulk solubility, the influence of surfactant–chelating agent interactions on surface and interfacial properties is equally important for formulation performance. In binary amphoteric–chelating agent systems, surface tension and contact angle measurements remain largely unchanged by the presence of GLDA. This suggests that the interaction occurs predominantly in the bulk phase, where increased surfactant hydrophilicity does not translate into enhanced surface activity. This observation is consistent with the fact that the less hydrophilic component dominates interfacial composition; in other words, weak interaction observed in binary systems, as discussed in earlier sections, will not promote interfacial activity.

Ternary systems selected to have comparable cloud points, ionic strengths, and pH values exhibit pronounced differences in surface wetting, foaming, and cleaning performance depending on the nature of the electrolyte, particularly when chelating agents are present. Contact angle measurements on hydrophobic soils show enhanced wetting over time for formulations containing a chelating agent compared to systems adjusted with NaCl and NaOH for similar ionic strength and pH (Figure 28). This behavior suggests that amphoteric–chelating agent interactions promote either the displacement of less hydrophilic surfactants to the interface or the formation of interfacial films that retain water more effectively, thereby promoting water uptake and swelling of the hydrophobic soil.

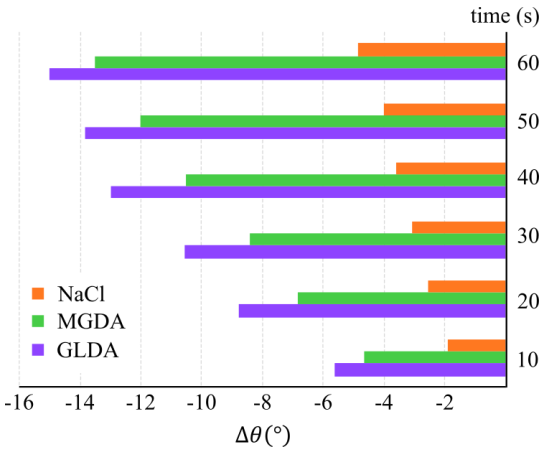

Figure 28. Time-dependent contact angle evolution for formulations containing a chelating agent, compared with reference formulations of identical surfactant composition, ionic strength, and pH adjusted using NaCl and NaOH.

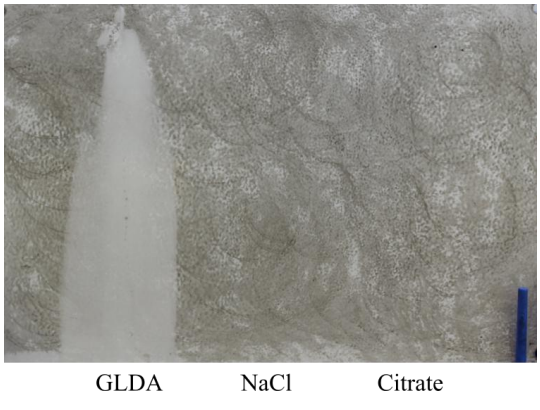

Figure 29. Comparative non-mechanical cleaning performance of formulations containing GLDA, sodium citrate, or NaCl at identical surfactant composition, ionic strength, and pH.

Consistent trends are observed in cleaning performance. Under equivalent pH and ionic strength conditions, formulations containing GLDA display significantly higher cleaning efficiencies than those containing NaCl or sodium citrate (Figure 29). While increasing ionic strength generally improves soil removal, the effect is most pronounced for GLDA-based systems, which exhibit measurable cleaning even at low ionic strength. Within these formulations, similar cleaning efficiencies are obtained at intermediate and high ionic strengths, corresponding to the interaction-saturated and salting-out regimes identified in the cloud point curves. At low ionic strength, however, cleaning efficiency decreases sharply, reflecting the strongly increased hydrophilicity of the system due to amphoteric–chelating agent interactions.

Oil incorporation follows a complementary pattern: in GLDA-containing dispersions, stability is maintained in the interaction-limited and interaction-saturated regimes, where chelating agent–surfactant interactions enhance headgroup hydration and micellar

organization, supporting stable emulsions. At higher chelating agent concentrations, corresponding to the salting-out regime, ionic effects dominate, reducing colloidal stability and leading to rapid oil separation.

Figure 30 summarizes the mechanistic basis of the observed trends in cleaning and oil incorporation, showing how chelating agent–induced changes in surfactant hydration, micellar structure, and bulk–interface partitioning control the balance between soil removal and oil dispersion across the different interaction regimes. In the interaction-limited regime, increased headgroup hydration favors solubilization of surfactant and oil in the bulk, limiting interfacial activity and reducing cleaning efficiency. In the interaction-saturated regime, maximal headgroup hydration and micellar restructuring promote dynamic exchange between bulk assemblies and interfaces, enabling efficient soil removal while maintaining stable emulsions. At higher chelating agent concentrations, corresponding to the salting-out regime, surfactant solubility decreases and interfacial partitioning increases, supporting rapid soil removal but destabilizing emulsions and accelerating phase separation.

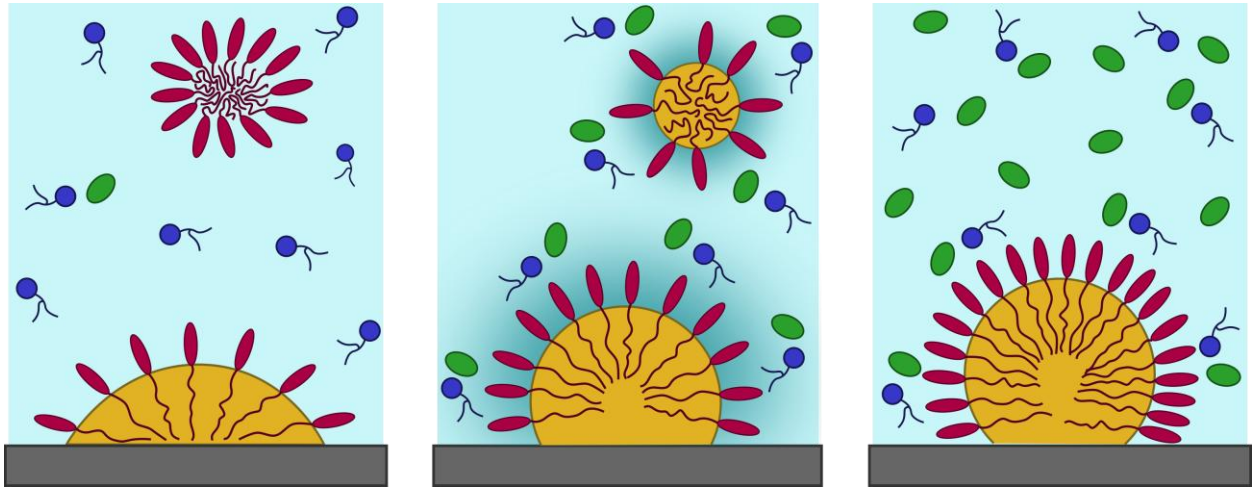

Figure 30. Mechanistic overview of soil removal and oil dispersion in amphoteric–chelating agent formulations, highlighting the role of surfactant hydration, micellar organization, and bulk–interface partitioning across the interaction-limited, interaction-saturated, and salting-out regimes. Red molecules represent nonionic surfactant, blue molecules amphoteric surfactant, and green molecules chelating agents, while yellow regions represent dirt or oily deposits.

Foam stability in GLDA-containing systems can also be interpreted using the identified surfactant–chelating agent regimes and the changes induced at the air–water interface. These systems exhibited reduced foam stability in the interaction-saturated regime, primarily due to increased spacing between surfactant headgroups caused by interactions with the amphoteric surfactant. The greater spacing weakens lamellae cohesion, accelerating foam decay.

Taken together, these macroscopic observations demonstrate that interactions between GLDA and amphoteric surfactants enhance interfacial activity in a manner that improves wetting, oil solubility, and cleaning efficiency while reducing foam stability. These coupled effects provide a coherent molecular-level explanation for formulation performance trends and underscore the central role of amphoteric–chelating agent interactions in controlling both bulk and interfacial behavior.

CHAPTER 5

Conclusions

Chelating agents are commonly treated as auxiliary components in surfactant formulations, valued primarily for their ability to bind metal ions while remaining otherwise inert. The results presented in this thesis challenge this assumption. Through a systematic, multi-scale investigation, this work demonstrates that chelating agents such as GLDA and MGDA can act as structure-directing additives, capable of reshaping micellar organization and altering formulation performance in ways that extend far beyond classical electrolyte effects.

At the molecular level, NMR techniques reveal that both GLDA and MGDA engage in dynamic interactions with micellar systems, despite lacking intrinsic self-assembly capabilities. These interactions are highly sensitive to surfactant architecture and are strongest in systems that can undergo substantial solubility changes driven by the minimization of hydrophobic interactions. The observed diffusion behavior reflects concentration-dependent exchange between bulk and micelle-associated environments, encompassing both fast and slow exchange regimes, with chelating agent association increasing with concentration until a saturation regime is reached. This response indicates that micellar systems

provide a finite number of favorable interaction environments, pointing to structure-specific interactions rather than a purely concentration-driven response.

The influence of chelating agents has consequences at the mesoscopic scale. Where, e.g., micellar diffusion reflects the molecular interactions described above. In systems containing linear amphoteric surfactants, efficient incorporation into mixed micelles enables pronounced reorganization upon chelating agent addition. For branched hydrophobic chains, packing flexibility is limited, restricting the extent to which chelating agent association can relieve hydrophobic or curvature-related penalties. Under these constraints, chelating agents do not induce substantial micellar growth or reshaping but instead promote a redistribution of surfactant components under dynamic exchange conditions, leading to more subtle changes in aggregate composition rather than morphology.

These structural changes manifest clearly in macroscopic formulation properties. Cloud point and viscosity measurements reveal regimes in which chelating agents counteract or even reverse classical salting-out behavior, particularly in amphoteric-stabilized systems. Such responses are consistent with reduced micellar size and increased solubility, directly linking macroscopic observables to micellar restructuring inferred from diffusion measurements.

The influence of chelating agents extends to interfacial and performance-related properties through their control of surfactant partitioning. Variations in wetting, cleaning efficiency, and foam stability in ternary systems are consistently governed by GLDA concentration, which regulates the balance between bulk solubilization and interfacial availability of the surfactant. Low chelating agent concentrations favor bulk partitioning and reduced interfacial activity, while higher concentrations induce salting-out effects that enhance surfactant adsorption at interfaces. These results show that chelating agents act as regulators

of surfactant distribution across interfaces, with clear relevance for formulation optimization.

Additionally, NMR techniques have enabled direct correlation of molecular-level dynamics with macroscopic formulation properties. By linking microscopic surfactant behavior to bulk observables, this approach demonstrates that widely accessible techniques such as cloud point determination, when interpreted within an appropriate structural framework, can provide deep insight into micellar behavior and support formulation development beyond purely empirical optimization.

In conclusion, this thesis redefines the role of chelating agents in surfactant systems. Rather than passive background components, chelating agents emerge as tunable, structure-sensitive additives that influence micellar organization, interfacial behavior, and formulation performance. Recognizing and exploiting this role opens new possibilities for rational formulation strategies in which chelating agents are deliberately chosen not only for regulating the effect of ions in solution, but also for their capacity to direct self-assembly and functional properties.

Future Perspectives

The present work has provided insight into the molecular interactions and aggregate behavior of mixed surfactant systems in the presence of chelating agents. Several avenues for future investigation emerge from these findings.

At the molecular level, the role of multivalent cations such as Ca^{2+} and Mg^{2+} on surfactant–chelating agent interactions merits further investigation. Their influence on surfactant–chelating agent interactions, aggregate structure, and chelation efficiency could be explored to better understand the behavior of formulations under hard water conditions.

The differences observed between surfactant architectures also point to opportunities for further investigation of molecular structure–property relationships. In binary systems, the branched amphoteric surfactant exhibited stronger interactions with the chelating agent than its linear analogue, while for linear surfactants the interaction strength followed the trend linear amphoteric > linear amine oxide > linear quaternary surfactant. Branched amine oxide and quaternary surfactants were not evaluated in the present work and represent a natural extension of this study. Furthermore, in ternary systems the linear amphoteric surfactant formed mixed micelles with the nonionic surfactant, with the presence of GLDA inducing micellar reshaping. Whether similar interaction-induced micellar restructuring could be observed for amine oxide–based systems, particularly in ternary formulations, remains an open question.

At the formulation level, cloud point measurements remain a valuable tool for probing phase behavior in mixed surfactant systems. Future work could examine correlations between cloud point and formulation concepts such as hydrophilic–lipophilic deviation, phase inversion temperature, and phase inversion composition, with the aim of improving predictive approaches for formulation design.

Together, these directions offer opportunities to deepen understanding of surfactant–chelating agent interactions, optimize formulation performance, and develop more predictive tools for complex cleaning systems.

Acknowledgment

The Swedish Foundation for Strategic Research and Nouryon Surface Chemistry AB are gratefully acknowledged for their financial support.

This work would not have been possible without the support and contributions of many people. I would like to begin by thanking my academic supervisors, Romain Bordes and Lars Evenäs, for their guidance, encouragement, and thoughtful challenges throughout this journey. Working with you has been both inspiring and rewarding, and I sincerely hope the feeling is mutual, because I fully intend to remain around.

I am also grateful to my industrial supervisors, Sorel Muresan and Ulf Schröder, as well as to my examiner, Martin Andersson, and the discussion leader of my Licentiate defense, Krister Holmberg, for their continued interest in my work, valuable discussions, and constructive input.

I would like to thank all co-authors and contributors who have been involved in this work, Sarah Lundgren, Alexander Idström, Clémence Le Coeur, Lorenzo Metilli, Anne-Laure Fameau, Louis Schwarzmayr, Emelie Nero, and Frida Jacobsson, for generating key data, engaging in insightful discussions, and for their support along the way.

A heartfelt thank you goes to everyone at Nouryon's Innovation Center in Stenungsund and at the Division of Applied Chemistry at Chalmers University of Technology for creating such welcoming, stimulating, and supportive environments in which to work.

Finally, I would like to thank my friends and family for their unwavering support. Most importantly, I thank my daughter, Salomé. You have shaped this journey in ways that go far beyond this thesis, and your influence is present in every step that led to its completion.

Bibliography

1. *Handbook of detergents. Part A: Properties.* vol. 82 (Marcel Dekker, Inc, New York, 1999).

2. Tan Tai, L. H. *Formulating detergents and personal care products.* (AOCS Press, Illinois, 2000).

3. *Handbook for cleaning/decontamination of surfaces.* vol. 1 (Elsevier, 2007).

4. Kronberg, B., Holmberg, K. & Lindman, B. *Surface chemistry of surfactants and polymers.* (John Wiley & Sons, Ltd., 2014). doi:10.1002/9781118695968.

5. Porter, M. R. *Handbook of surfactants.* (Springer, 2013).

6. Rosen, M. J. & Kunjappu, J. T. *Surfactants and interfacial phenomena.* (John Wiley & Sons., 2012). doi:10.1002/9781118228920.

7. Evans, D. F. & Wennerstroem, H. *The colloidal domain where physics, chemistry and biology meet.* (Willey-VCH, 1999).

8. van Zanten, R. Stabilizing viscoelastic surfactants in high-density brines. *SPE Drilling & Completion* 26, 499–505 (2011).

9. Nagarajan, R. Molecular packing parameter and surfactant self-assembly: The neglected role of the surfactant tail. *Langmuir* 18, 31–38 (2002).

10. Ginn, M. E. & Harris, J. C. Correlation between critical micelle concentration, fatty soil removal, and solubilization. *J. Am. Oil Chem. Soc.* 38, 605–609 (1961).

11. Mankowich, A. M. Hard surface detergency. *J. Am. Oil Chem. Soc.* 38, 589–594 (1961).

12. Raney, K. H. Optimization of nonionic/anionic surfactant blends for enhanced oily soil removal. *J. Am. Oil Chem. Soc.* 68, (1991).

13. Raney, K. H. & Benson, H. L. The effect of polar soil components on the phase inversion temperature and optimum detergency conditions. *J. Am. Oil Chem. Soc.* 67, 722–729 (1990).

14. Raney, K. H., Benton, W. J. & Miller, C. A. Optimum detergency conditions with nonionic surfactants. I. Ternary water-surfactant-hydrocarbon systems. *J. Colloid Interface Sci.* 117, 282–290 (1987).

15. Thompson, L. The role of oil detachment mechanisms in determining optimum detergency conditions. *J. Colloid Interface Sci.* 163, 61–73 (1994).

16. Shinoda, K. & Arai, H. The correlation between phase inversion temperature in emulsion and cloud point in solution of nonionic emulsifier. *J. Phys. Chem.* 68, 3485–3490 (1964).

17. Rojvoranun, S., Chavadej, S., Scamehorn, J. F. & Sabatini, D. A. Mechanistic studies of particulate soil detergency: II: Hydrophilic soil removal. *J. Surfactants Deterg.* 15, 663–677 (2012).

18. Rojvoranun, S. *et al.* Mechanistic studies of particulate soil detergency: I. Hydrophobic soil removal. *J. Surfactants Deterg.* 15, 277–289 (2012).

19. Holmberg, K. Surfactants. in *Ullmann's Encyclopedia of Industrial Chemistry* 1–56 (Wiley-VCH Verlag GmbH & Co. KGaA, Weinheim, Germany, 2019). doi:10.1002/14356007.a25_747.pub2.

20. Prieto, N. E., Lilienthal, W. & Tortorici, P. L. Correlation between spray cleaning detergency and dynamic surface tension of nonionic surfactants. *J. Am. Oil Chem. Soc.* 73, 9–13 (1996).

21. Schad, T. *et al.* Less is more: Unstable foams clean better than stable foams. *J. Colloid Interface Sci.* 590, 311–320 (2021).

22. Schad, T., Preisig, N., Drenckhan, W. & Stubenrauch, C. Foam-based cleaning of surfaces contaminated with mixtures of oil and soot. *J. Surfactants Deterg.* 25, 377–385 (2022).

23. Stubenrauch, C. & Drenckhan, W. Cleaning solid surfaces with liquid interfaces and foams: From theory to applications. *Curr. Opin. Colloid Interface Sci.* 72, 101818 (2024).

24. Bauduin, P., Renoncourt, A., Kopf, A., Touraud, D. & Kunz, W. Unified concept of solubilization in water by hydrotropes and cosolvents. *Langmuir* 21, 6769–6775 (2005).

25. Zemb, T. N. *et al.* How to explain microemulsions formed by solvent mixtures without conventional surfactants. *Proceedings of the National Academy of Sciences* 113, 4260–4265 (2016).

26. Jiang, J. & Williams III, R. O. Cosolvent and Complexation Systems. in *Formulating poorly water soluble drugs* (eds. Williams III, R. O., Davis Jr., D. A. & Miller, D. A.) 179–217 (Springer, Cham, Switzerland, 2022).

27. Smith, P. E. & Mazo, R. M. On the theory of solute solubility in mixed solvents. *J Phys Chem B* 112, 7875–7884 (2008).

28. Jouyban, A. Review of the cosolvency models for predicting solubility of drugs in water-cosolvent mixtures. *Journal of Pharmacy and Pharmaceutical Sciences* 11, 32–58 (2008).

29. Neuberg, Carl. Hydrotropic appearances. *Biochem.Z* 76, 107–108 (1916).

30. Friberg, S. E. Hydrotropes. *Curr. Opin. Colloid Interface Sci.* 2, 490–494 (1997).

31. González, G., Nassar, E. J. & Zaniquelli, M. E. D. Examination of the hydrotropic effect of sodium p-toluenesulfonate on a nonionic surfactant ($C_{12}E_6$) solution. *J. Colloid Interface Sci.* 230, 223–228 (2000).

32. Kunz, W., Holmberg, K. & Zemb, T. Hydrotropes. *Curr. Opin. Colloid Interface Sci.* 22, 99–107 (2016).

33. Eastoe, J., Hatzopoulos, M. H. & Dowding, P. J. Action of hydrotropes and alkyl-hydrotropes. *Soft Matter* 7, 5917–5925 (2011).

34. Hopkins Hatzopoulos, M. *et al.* Are hydrotropes distinct from surfactants? *Langmuir* 27, 12346–12353 (2011).

35. Zhao, W. *et al.* Aggregation of a cationic gemini surfactant with a chelating molecule and effects from calcium ions. *Langmuir* 33, 12719–12728 (2017).

36. Soontravanich, S., Lopez, H. E., Scamehorn, J. F., Sabatini, D. A. & Scheuing, D. R. Dissolution study of salt of long chain fatty acids (soap scum) in surfactant solutions. Part I: Equilibrium dissolution. *J. Surfactants Deterg.* 13, 367–372 (2010).

37. Yunusov, T. I., Davletshina, L. F., Magadova, L. A. & Silin, M. A. Study of chelating agent-surfactant interactions on the interphase as possibly useful for the well stimulation. *Energies (Basel).* 16, 1679 (2023).

38. Yan, Z., Liu, L., Chen, X. & Niu, Y. Physicochemical studies on molecular interactions between small biomolecules and drug benzalkonium chloride at different temperatures T = (293.15–313.15) K. *J. Mol. Liq.* 274, 115–124 (2019).

39. Chauhan, S. & Sharma, K. Effect of temperature and additives on the critical micelle concentration and thermodynamics of micelle formation of sodium dodecyl benzene sulfonate and dodecyltrimethylammonium bromide in aqueous solution: A conductometric study. *Journal of Chemical Thermodynamics* 71, 205–211 (2014).

40. Kandpal, N. D., Joshi, S. K., Singh, R. & Pandey, K. Thermodynamic parameters of micellization and transfer of amino acid from water to aqueous linear alkyl benzene sulphonate. *J. Indian Chem. Soc.* 87, 487–493 (2010).

41. Otzen, D. Protein-surfactant interactions: A tale of many states. *Biochim. Biophys. Acta* 1814, 562–591 (2011).

42. Malik, N. A. Surfactant–amino acid and surfactant–surfactant interactions in aqueous medium: a review. *Appl. Biochem. Biotechnol.* 176, 2077–2106 (2015).

43. Singh Raman, A. P. *et al.* A review on interactions between amino acids and surfactants as well as their impact on corrosion inhibition. *ACS Omega* 7, 47471–47489 (2022).

44. Deng, X. *et al.* Wettability alteration of carbonate rock by chelating agents and viscoelastic surfactants: synergetic impact. *Energy and Fuels* 36, 7391–7401 (2022).

45. Hassan, A. *et al.* Applications of chelating agents in the upstream oil and gas industry: A review. *Energy and Fuels* 34, 15593–15613 (2020).

46. Hazrina, H. Z., Noorashikin, M. S., Beh, S. Y., Loh, S. H. & Zain, N. N. M. Formulation of chelating agent with surfactant in cloud point extraction of methylphenol in water. *R. Soc. Open Sci.* 5, (2018).

47. Muresan, S., Velásquez, J. & Borgland, O. Chelate-amphoteric surfactant liquid concentrates and use thereof in cleaning applications. (2023).

48. Wennerström, H. & Lindman, B. Micelles, Physical Chemistry of Surfactant Association. *Physics Reports (Review Section of Physics Letters)* 52, 1–86 (1979).

49. Cui, X., Mao, S., Liu, M., Yuan, H. & Du, Y. Mechanism of surfactant micelle formation. *Langmuir* 24, 10771–10775 (2008).

50. Persson, B.-O., Drakenberg, T. & Lindman, B. Amphiphile aggregation number and conformation from carbon-13 nuclear magnetic resonance chemical shifts. *J. Phys. Chem.* 80, 2124–2125 (1976).

51. Persson, B.-O., Drakenberg, T. & Lindman, B. ^{13}C NMR of micellar solutions. Micellar aggregation number from the concentration dependence of the ^{13}C chemical shifts. *J. Phys. Chem.* 83, 3011–3015 (1979).

52. Waudby, C. A. & Alfonso, I. An introduction to one- and two-dimensional lineshape analysis of chemically exchanging systems. *J. Magn. Reson. Open* 16–17, 100102 (2023).

53. Waudby, C. A. & Christodoulou, J. NMR lineshape analysis of intrinsically disordered protein interactions. in *Intrinsically disordered proteins: methods and protocols* 477–504 (Springer New York, New York, 2020). doi:10.1007/978-1-0716-0524-0_24.

54. Barhoum, S., Palit, S. & Yethiraj, A. Diffusion NMR studies of macromolecular complex formation, crowding and confinement in soft materials. *Prog. Nucl. Magn. Reson. Spectrosc.* 94–95, 1–10 (2016).

55. Stilbs, P. & Lindman, B. Determination of organic counterion binding to micelles through Fourier transform NMR self-diffusion measurements. *J. Phys. Chem* 85, 2587–2589 (1981).

56. Groves, P. Diffusion ordered spectroscopy (DOSY) as applied to polymers. *Polym. Chem.* 8, 6700–6708 (2017).

57. Colafemmina, G., Mateos, H. & Palazzo, G. Diffusion NMR studies of complex liquid formulations. *Curr. Opin. Colloid Interface Sci.* 48, 109–120 (2020).

58. Furó, I. NMR spectroscopy of micelles and related systems. *J. Mol. Liq.* 117, 117–137 (2005).

59. Johnson, C. S. Diffusion ordered nuclear magnetic resonance spectroscopy: principles and applications. *Prog. Nucl. Magn. Reson. Spectrosc.* 34, 203–256 (1999).

60. Bijma, K. & Engberts, J. B. F. N. Effect of counterions on properties of micelles formed by alkylpyridinium surfactants. 1. Conductometry and ^{1}H-NMR chemical shifts. *Langmuir* 13, 4843–4849 (1997).

61. Andrade-Dias, C., Lima, S. & Teixeira-Dias, J. J. C. From simple amphiphilic to surfactant behavior: Analysis of ^{1}H NMR chemical shift variations. *J. Colloid Interface Sci.* 316, 31–36 (2007).

62. Yuan, H. Z. *et al.* Aggregation of sodium dodecyl sulfate in poly(ethylene glycol) aqueous solution studied by ^{1}H NMR spectroscopy. *Colloid Polym. Sci.* 280, 479–484 (2002).

63. Dong, S., Xu, G. & Hoffmann, H. Aggregation behavior of fluorocarbon and hydrocarbon cationic surfactant mixtures: A study of ^{1}H NMR and ^{19}F NMR. *J. Phys. Chem. B* 112, 9371–9378 (2008).

64. Okano, L. T., El Seoud, O. A. & Halstead, T. K. A proton NMR study on aggregation of cationic surfactants in water: effects of the structure of the headgroup. *Colloid Polym. Sci.* 275, 138–145 (1997).

65. Rufier, C., Collet, A., Viguier, M., Oberdisse, J. & Mora, S. SDS interactions with hydrophobically end-capped poly(ethylene oxide) studied by ^{13}C NMR and SANS. *Macromolecules* 42, 5226–5235 (2009).

66. Petit-Agnely, F. & Iliopoulos, I. Aggregation mechanism of amphiphilic associating polymers studied by ^{19}F and ^{13}C nuclear magnetic resonance. *J. Phys. Chem. B* 103, 4803–4808 (1999).

67. Rosenholm, J. B., Drakenberg, T. & Lindman, B. A Carbon-13 NMR shielding study of the water-sodium octanoate-pentanol, and water-sodium octanoate-decanol systems. *J. Colloid Interface Sci.* 63, 538–550 (1978).

68. Muller, N. & Simsohn, H. Investigation of micelle structure by fluorine magnetic resonance. V. Sodium Perfluorooctanoate. *J. Phys. Chem.* 75, 942–945 (1971).

69. Amato, M. E., Caponetti, E., Chillura Martino, D. & Pedone, L. ^{1}H and ^{19}F NMR investigation on mixed hydrocarbon-fluorocarbon micelles. *J. Phys. Chem. B* 107, 10048–10056 (2003).

70. Nordstierna, L. Molecular association studied by NMR spectroscopy. (KTH, Stockholm, 2006).

71. Ross Hallett, F. Scattering and particle sizing applications. in *Encyclopedia of Spectroscopy and Spectrometry* 2488–2494 (Elsevier, 1999). doi:10.1016/B978-0-12-374413-5.00277-3.

72. Kumar, A. & Dixit, C. K. Methods for characterization of nanoparticles. in *Advances in Nanomedicine for the Delivery of Therapeutic Nucleic Acids* 43–58 (Elsevier, 2017). doi:10.1016/B978-0-08-100557-6.00003-1.

73. Windsor, C. G. An introduction to small-angle neutron scattering. *J. Appl. Crystallogr.* 21, 582–588 (1988).

74. Hollamby, M. J. Practical applications of small-angle neutron scattering. *Physical Chemistry Chemical Physics* 15, 10566–10579 (2013).

75. Porte, G. Micellar growth, flexibility and polymorphism in dilute solutions. in *Micelles, membranes, microemulsions, and monolayers* 105–151 (Springer Netherlands, New York, 1994). doi:10.1007/978-1-4613-8389-5_2.

76. Kanicky, J. R. & Shah, D. O. Effect of degree, type, and position of unsaturation on the pKa of long-chain fatty acids. *J. Colloid Interface Sci.* 256, 201–207 (2002).

77. Kanicky, J. R. & Shah, D. O. Effect of premicellar aggregation on the pKa of fatty acid soap solutions. *Langmuir* 19, 2034–2038 (2003).

78. Li, Y., Holmberg, K. & Bordes, R. Micellization of true amphoteric surfactants. *J. Colloid Interface Sci.* 411, 47–52 (2013).

79. Koch, D. *et al.* The analysis of electron densities: From basics to emergent applications. *Chem. Rev.* 124, 12661–12737 (2024).

80. Zhang, Q. *et al.* Synthesis, aggregation behavior and interfacial activity of branched alkylbenzenesulfonate gemini surfactants. *J. Colloid Interface Sci.* 362, 406–414 (2011).

81. Mirzamani, M. *et al.* Structural alterations of branched versus linear mixed-surfactant micellar systems with the addition of a complex perfume mixture and dipropylene glycol as cosolvent. *RSC Adv.* 12, 14998–15007 (2022).

82. Cheng, L. & Cao, D. Effect of tail architecture on self-assembly of amphiphiles for polymeric micelles. *Langmuir* 25, 2749–2756 (2009).

83. Shrestha, L. K., Sato, T., Dulle, M., Glatter, O. & Aramaki, K. Effect of lipophilic tail architecture and solvent engineering on the structure of trehalose-based nonionic surfactant reverse micelles. *Journal of Physical Chemistry B* 114, 12008–12017 (2010).